SIMPLIFIED INELASTIC ANALYSIS OF NOTCHED COMPONENTS SUBJECTED TO MECHANICAL AND THERMAL LOADS

PRASANNA RAGHAVAN

INFORMATION TO USERS

This manuscript has been reproduced from the microfilm master. UMI films the text directly from the original or copy submitted. Thus, some thesis and dissertation copies are in typewriter face, while others may be from any type of computer printer.

The quality of this reproduction is dependent upon the quality of the copy submitted. Broken or indistinct print, colored or poor quality illustrations and photographs, print bleedthrough, substandard margins, and improper alignment can adversely affect reproduction.

In the unlikely event that the author did not send UMI a complete manuscript and there are missing pages, these will be noted. Also, if unauthorized copyright material had to be removed, a note will indicate the deletion.

Oversize materials (e.g., maps, drawings, charts) are reproduced by sectioning the original, beginning at the upper left-hand corner and continuing from left to right in equal sections with small overlaps. Each original is also photographed in one exposure and is included in reduced form at the back of the book.

Photographs included in the original manuscript have been reproduced xerographically in this copy. Higher quality 6" x 9" black and white photographic prints are available for any photographs or illustrations appearing in this copy for an additional charge. Contact UMI directly to order.

NOTE TO USERS

The original manuscript received by UMI contains pages with indistinct print.   Pages were microfilmed as received.

This reproduction is the best copy available

UMI

SIMPLIFIED INELASTIC ANALYSIS OF NOTCHED COMPONENTS SUBJECTED TO MECHANICAL AND THERMAL LOADS

By

Prasanna Raghavan, B.E

A THESIS

SUBMITTED TO THE SCHOOL OF GRADUATE STUDIES

IN PARTIAL FULFILLMENT OF THE REQUIREMENTS

FOR THE DEGREE OF

MASTER OF ENGINEERING

FACULTY OF ENGINEERING AND APPLIED SCIENCE

MEMORIAL UNIVERSITY OF NEWFOUNDLAND

St. John's, Newfoundland, Canada

September 1998

0-612-36170-5

Canada

Abstract

Estimation of inelastic strains in notched mechanical components and structures are necessary for low cycle fatigue evaluations. This has been a topic of considerable interest to pressure vessel designers.

The Generalized Local Stress Strain (GLOSS) method is a robust technique that is based on two linear elastic finite element analyses, and has been used for evaluating *inelastic strains in pressure components subjected to mechanical loadings. This thesis* endeavors to determine the inelastic strains of components and structures that are subjected to both mechanical as well as thermal loadings. A two bar kinematic model is used to explain the fundamental aspects of modulus reduction method. Using the elastic-inelastic equivalence, a procedure to obtain the complete relaxation locus has been provided. Based on the relaxation locus, the GLOSS method is extended for combined mechanical and thermal loadings.

In this thesis, GLOSS method is applied to several pressure component configurations of practical interest. The strain estimates are then validated by comparing them with inelastic finite element results.

Acknowledgements

Dedication

Dedicated to my grandmothers Shrimathi. S. Sundaravalli and Shrimathi. K. Booma.

Contents

List of Figures

List of Tables

Nomenclature

B, n	creep parameters for second stage power law creep
E	modulus of elasticity
$\bar{E}_r$	normalized relaxation-modulus
E_s	secant-modulus
E_r	relaxation-modulus
A_1, A_2	cross-sectional area of bar one and two respectively
A_k	area (kth element)
E_1, E_2	modulus of elasticity of bar one and two respectively
I_1, I_2, I_3	invariants of the stress tensor
J_1, J_2, J_3	invariants of the deviatoric stress tensor
L_1, L_2	length of bar one and two respectively
P	applied external load
P_y	yield initiation load of the componenet
P_L	limit load of the componenet
S	nominal or remote stress in a component
S_i	sum of forces under the area ($i = 1..6$)
S_T	surface area of a structure over which traction is prescribed
S_u	surface on which displacement is prescribed
V	volume of a component or structure
W_S	strain energy per unit volume of the remote region

W_σ	strain energy per unit volume of the local region
a	radius of the circular hole in a thin plate
b	width of a thin plate
k_t	stress concentration factor in elastic case
k_ϵ	plastic strain concentration factor
k_σ	plastic stress concentration factor
k_p	plastic limit load factor
α_1, α_2	coefficient of thermal expansion of bar one and two respectively
$\Delta T_1, \Delta T_2$	rise in temperature of bar one and two respectively
δ	net deformation of the two bars
δ_{ij}	Kronecke delta
γ	softening parameter
$\bar{\lambda}$	constraint parameter
ν	Poisson's ratio
ν_s	modified Poisson's ratio
θ	follow-up angle on the GLOSS diagram
$\dot{\epsilon}$	strain rate
ϵ_{eqv}	total equivalent strain
ϵ_n	notch root strain
$\epsilon_{1e}, \epsilon_{2e}$	elastic strain in bar one and two respectively
$\epsilon_{t1}, \epsilon_{t2}$	total strain in bar one and two respectively
$\epsilon_{1\theta}, \epsilon_{2\theta}$	thermal strain in bar one and two respectively
σ_R	reference stress
σ_1, σ_2	axial stress in bar one and two respectively
σ_i	principal stresses ($i = 1..3$)
σ'_{ij}	deviatoric stress tensor

σ_{ek}	equivalent stress (kth element)
σ_m	mean or hydrostatic stress
σ_n	notch root stress
σ_y	yield stress

Acronyms and Abbreviations

ADPL	ANSYS Design Parametric Language [2]
FEA	Finite Element Analysis
GLOSS	Generalized Local Stress Strain
GMPC	GLOSS method with Plasticity Correction

Chapter 1

Introduction

1.1 General Background

Ensuring performance, safety and durability are some of the key objectives in designing any component, while keeping cognizance of the economy of design and operational costs. A clear understanding of the various modes of structural failures helps the design process to be more rational and economical in the long term. While prototype and component testing are often necessary to verify the integrity of components, the time and cost involved makes them less attractive to designers. With the advent of high speed digital computers, various modes of failures can be studied, thereby speeding up the design process.

Failures due to excessive plastic deformation, fatigue, fracture and creep are some of the common modes of failure. The process of designing components to avoid failure due to low-cycle fatigue and the means of carrying out such a design is the topic of interest in this thesis. Fatigue is a process which causes damage of a component subjected to repeated loading. Primary fatigue analysis methods are the stress life approach, the strain life approach and the fracture mechanics approach. The stress life approach is widely used in design applications where the stresses in the component are primarily within the elastic range of the material and the cycles to failure are long.

1

Geometric discontinuities such as holes. fillets and grooves that are unavoidable in design cause stress to be locally elevated and are potential fatigue crack initiation locations. Such notched components are often subjected to loads causing local yielding at the notch root. It is convenient to separate the total fatigue life of notched members into two portions: firstly the crack initiation life. which is spent in nucleating small cracks. and secondly the crack propagation life. which is spent in growing these cracks to final fracture. While the cyclic plastic strain at the notch root is the controlling factor during the early stages of fatigue life, nominal stress and crack length are the controlling factors during the later stages.

Strain life concepts are used to estimate the fatigue life when notch root plasticity is the controlling parameter. Equivalent fatigue failure is assumed to occur in the material at the notch root and in the smooth specimen when both are subjected to identical stress-strain histories.

Since closed form solutions are not easy to obtain for the inelastic problem. numerical methods are often resorted to. Non-linear finite element analysis, although it provides reasonable results. is quite often elaborate. time consuming and expensive. The use of nonlinear elasto-plastic stress-strain relationships makes the analysis more complex when compared to linear elastic analysis. Further. the large amount of output data has to be properly interpreted in order to get meaningful results from the analysis. Consequently, there is a need for simple methods to determine the inelastic behavior of components.

1.2   Need for Robust Methods

One of the more widely used approximate method to determine the inelastic strain is Neuber's rule [23]. In this method nominal stress and strain are related to the local counterparts. It requires the use of a single elastic finite element analysis or a linear

elastic analytical solution. This method, initially developed for torsional loadings, was then applied to plane stress configurations. The strain estimated by Neuber's rule was found by Mowbray [22] to be reasonably accurate for plane stress cases. The life estimates have been found to be very conservative for situations other than plane stress. In particular, the effect of multiaxiality is not properly considered.

Keeping cognizance of the importance of inelastic strain assessment and the inadequacy of the existing methods, this thesis endeavors to develop a generic robust method based on two linear elastic finite element analyses for an inelastic evaluation of notched components and structures subjected to combined mechanical and thermal loadings.

In the context of this thesis, robustness implies the ability to provide acceptable results based on less than reliable input together with conceptual insight and economy of computational effort [29]. Robust methods are suitable for

- initial scoping and feasibility study

- screening of critical situations in large complex systems for further detailed analysis

- "sanity" checks on results obtained by detailed inelastic analysis

- approximate estimate of inelastic effects

Robust methods are especially appropriate for assessments in an operating plant environment where detailed characterization of material damage is difficult to obtain. In such situations robust approximate methods would provide reasonable assessment of the condition of equipment or systems.

1.3 Organization of the Thesis

The need for robust methods of inelastic strain estimation in notched components is addressed in Chapter 1. The cost and time constraints posed by nonlinear finite element analysis, and the overly conservative Neuber's rule have necessitated robust approximate methods. The objectives and the organization of the thesis are also presented in this chapter.

Chapter 2 discusses the basic concepts in plasticity and fatigue. An incremental iterative algorithm for the numerical solution of elasto-plastic problems is presented. Existing approximate methods for the determination of notch root strains such as Neuber's rule [23] and Molski-Glinka method [20] are discussed. The extension of Neuber's rule to account for bending and non-linear nominal stress range using a limit load factor developed by Seeger and Heuler [28] is described. A discussion of the methods developed by Hoffman and Seeger [13] and Glinka et. al. [21] to determine the multiaxial notch root elasto-plastic stresses and strains is carried out.

The concept of multiaxial stress relaxation is introduced in Chapter 3. Multiaxial relaxation and uniaxial relaxation are related through the constraint parameter by Seshadri and Mikulcik [36]. It has been shown that the constraint parameter can be expressed as a function of principal stress and strain ratios for any location in a structure. As a consequence of the aforementioned ideas, GLOSS (Generalized Local Stress Strain) method was introduced by Seshadri [29] as a practical technique to determine the constraint parameter and local region inelastic strain for any general component. In this method, a finite element analysis is carried out by assuming that the component is linear elastic. The moduli of all the elements that are above yield are modified in the second linear elastic finite element analysis in a systematic manner in order to simulate the inelastic behavior. To account for proper plastic zone size, Seshadri and Kizhatil [34] developed the GLOSS method with Plasticity

4

Correction. The method is developed based on equilibrium considerations leading to better inelastic strain estimates.

The basic concepts of modulus reduction method are elaborated in Chapter 4 by using a two bar model for the purpose of illustration. It is shown that, in principle, the constraint parameter is independent of the amount of softening of the local bar elastic modulus for the two bar model subjected to combined mechanical and thermal loadings. Analytical expressions show that the local bar strain predicted by the inelastic analysis and modulus modification method are equal.

Chapter 5 describes the procedure for determining the complete relaxation locus using inelastic finite element analysis. It is shown that any inelastic distribution can be obtained with an elastic analysis provided the modulus of elasticity and Poisson's ratio of every element are known. Using this equivalence, the complete relaxation locus can be determined from an inelastic finite element analysis. The local as well as remote relaxation locus obtained from inelastic finite element analysis is studied for the two bar model and for some general mechanical components subjected to mechanical and thermal loadings. A modified modulus adjustment technique for combined loadings is also presented.

The proposed method for determining the inelastic strains is applied to typical pressure component configurations in Chapter 6. A plate with a hole, a Bridgman notch, a cylinder with a circumferential notch on the inside surface and an industrial steam turbine valve body are the specific components that are analyzed. The pressure components are subjected to mechanical as well as thermal loadings. Cyclic effects due to pressure and temperature resulting from unit start-up, operation and shut-down, which can lead to possible ratchetting and low cycle fatigue are of design interest. The valve body is analyzed for a range of start-up rates and the resulting maximum temperature difference at a given critical section is determined. Using this

temperature distribution, a stress analysis is performed in order to determine the maximum possible inelastic strain range. Results obtained from the GLOSS method with Plasticity Correction are compared with those obtained from inelastic finite element analyses and Neuber's rule.

The main contributions of the research work are presented in Chapter 7. A case is made here for the attractiveness of robust methods of design and analysis in the context of industrial applications.

ANSYS [2] input files for performing linear as well as non-linear finite element analysis are given in Appendix A. The GLOSS method with Plasticity Correction and the process of inelastic stress relaxation have been coded in the form of ADPL (ANSYS Design Parametric Language) macros within ANSYS. The macros listings are given in Appendix B.

Chapter 2

Literature Review

2.1 Problem Formulation in Solid Mechanics

Formulation of a boundary value problem in solid mechanics involves the determination of the distribution of stresses and strains in the interior of the body for a prescribed traction distribution over a part of the boundary, and a prescribed displacement distribution over a different part of the boundary. For a body with volume V and surface area S subjected to body forces f_i in V, surface forces T_i on S_T, and prescribed displacements u_i^o on S_u (Fig. 2.1), the equations of equilibrium are given by

$$\sigma_{ij,j} + f_i = 0 \quad \text{in } V. \tag{2.1}$$

Based on the small displacement theory the strain-displacement or kinematic relations can be expressed as

$$\epsilon_{ij} = \frac{1}{2} \left(u_{i,j} + u_{j,i} \right) \quad \text{in } V. \tag{2.2}$$

Tractions are specified on the surface in the form of point loads, distributed load and moments. In general, however, the equations can be expressed as

$$\sigma_{ij} n_j = T_i \quad \text{on } S_T$$

$$u_i = u_i^o \quad \text{on } S_u. \tag{2.3}$$
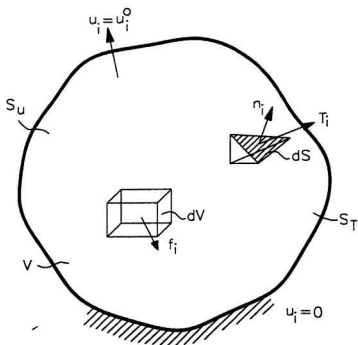
Figure 2.1: Body under traction forces

Finally, the stresses and strains are related through constitutive equations, which could depend on the strain rate and temperature, and can be written as

$$\sigma_{ij} = f\left(\epsilon_{ij}, \dot{\epsilon}_{ij}, T\right). \qquad (2.4)$$

While the relationship between the stress and strain is linear in the elastic range, it is non-linear in the plastic range. Closed form analytical solutions are difficult to obtain in the plastic range, which necessitates the use of numerical methods such as the finite element method. Theoretical aspects pertaining to elastic-plastic analysis, finite element method and approximate methods in notched component analysis are presented in this chapter.

2.2 Material Stress-Strain Curve

The stress-strain relation of a material is obtained from a uniaxial tensile test. A typical stress-strain diagram for a number of metals and alloys is shown in Fig. 2.2. The portion of the curve OA showing the relation between the stress and the strain, is linear. Stress and strain are proportional though a constant called the modulus of elasticity which is essentially a material property. In the elastic range

- stresses and strains are related through Hooke's Law

- the strains are path independent

- there is complete reversibility of stresses occurs during the unloading process.

The point A is identified as the yield point which demarcates the linear and the nonlinear range of the behavior. On further increases in the applied load, the stress-strain curve follows the path AB which is nonlinear. As the deformation continues, the stress required also increases indicating the resistance of the material to further plastic deformation. The stress required to produce this further plastic deformation is

9
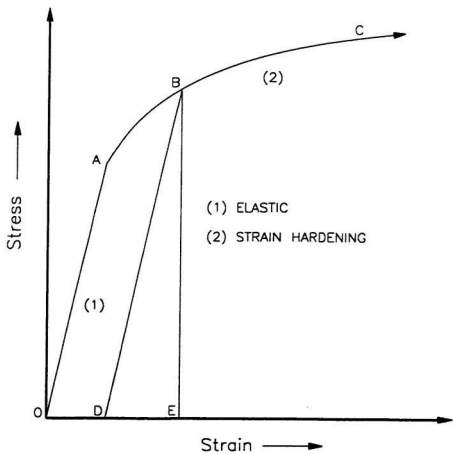
Figure 2.2: Material Stress-Strain Curve

usually referred to as the flow stress. Stresses and strains are no longer proportional. therefore. there is a need to characterize plastic behavior through more appropriate constitutive equations. In the plastic range

- the strains are irrecoverable

- the stresses and strains are path and. therefore. history dependent

- hydrostatic state of stress has no effect on yielding

- the material is assumed to be incompressible (Poisson ratio = 0.5)

- the stress and strains are related through "flow rules"

- effect of strain rate is negligible

If the material is stressed up to point B and then unloaded, the unloading path is considered to be linear. It follows the path BD which is parallel to the line OA. The net strain is comprised of two parts. The portion OD is the irrecoverable plastic strain and the portion DE is the recoverable elastic strain. If the specimen is reloaded again, the unloading path DB is more or less retraced. Plastic flow does not occur until the point B is reached after which plastic strain is induced. Thereafter, the rest of the stress–strain curve BC is traced.

The material stress-strain curve can be idealized (Fig. 2.3) in number of ways.

- **Elastic Perfectly Plastic Model**

    The material is assumed to follow the Hooke's Law until the yield point is reached after which the strain is assumed to increase without any bound. The model assumes that the structure made of this material cannot take any more load, once the stress reaches the yield. This model is widely used as it is simple to use in practice.

11
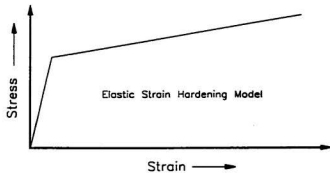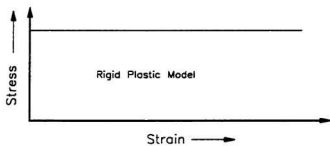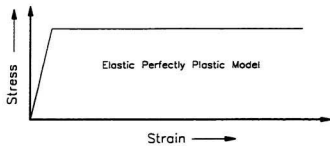
Figure 2.3: Material Models

- **Rigid Perfectly Plastic Model**

  When elastic strains are small compared to plastic strains, this model is appropriate. Deformations are not induced until the stresses reach the yield beyond which the strains are unbounded. This model is particularly useful in determining limit loads of structures and in metal forming operations.

- **Elastic Linear Strain Hardening Model**

  This model is an approximation for stress strain curves that rise after yielding. It is bilinear in the sense that the strain hardening portion of the model is also linear but with a different slope.

2.3 Multiaxial State of Stress

The state of stress in any general mechanical component is usually multiaxial. In order to determine the elastic limit due to a given three dimensional stress state. a yield criterion is required. For isotropic materials, it is required that the failure criterion be independent of the choice of the coordinate system. The yield function (ϕ) would therefore depend on the stress invariants [19].

$$\phi\left(I_1, I_2, I_3\right) = 0 \tag{2.5}$$

where the stress invariants I_1, I_2, I_3 are

$$
\begin{aligned}
I_1 &= \sigma_1 + \sigma_2 + \sigma_3 \\
I_2 &= -\left(\sigma_1\sigma_2 + \sigma_2\sigma_3 + \sigma_3\sigma_1\right) \\
I_3 &= \sigma_1\sigma_2\sigma_3.
\end{aligned}
\tag{2.6}
$$

It has been shown experimentally by Bridgman and others [12, 19] that moderate hydrostatic stress state (either compressive or tensile), does not affect the yield. The

13

stress tensor can be decomposed into a hydrostatic stress tensor and a deviatoric stress tensor. The hydrostatic stress tensor is a tensor whose elements are $\sigma_m \delta_{ij}$. where σ_m is the mean stress, i.e.,

$$p_{ij} = \sigma_m \delta_{ij} = \frac{1}{3}(\sigma_1 + \sigma_2 + \sigma_3) = \frac{1}{3}I_1 \qquad (2.7)$$

δ_{ij} is the Kronecker Delta and is equal to 1 if $i = j$ and 0 if $i \neq j$. The deviatoric stress tensor (s_{ij}) is defined by subtracting the hydrostatic state of stress from the actual state of stress (σ_{ij}). Mathematically, deviatoric stress tensor is given by

$$s_{ij} = \sigma_{ij} - \frac{1}{3}\sigma_{kk}\delta_{ij}. \qquad (2.8)$$

Since the hydrostatic stresses does not affect yielding, the yield criterion can then be expressed in terms of the invariants of the deviatoric stress tensor as

$$\phi(J_1, J_2, J_3) = 0 \qquad (2.9)$$

where J_1, J_2, J_3 are related to the invariants I_1, I_2 and I_3 of the stress tensor σ_{ij} through the following relations.

$$\begin{aligned} J_1 &= 0 \\ J_2 &= \frac{1}{3}\left(I_1^2 + 3I_2\right) \\ J_3 &= \frac{1}{27}\left(2I_1^3 + 9I_1I_2 + 27I_3\right). \end{aligned} \qquad (2.10)$$

The two of the most commonly used yield criterion are the von Mises yield criterion and the Tresca yield criterion.

In an elastic material, the applied stress is stored as internal strain energy. A portion of the energy is associated with a change in volume and the remaining is associated with distorting the shape of the material. Hydrostatic stress is associated with dilation or volume change, and does not affect the yielding. Since the distortional

14

energy is proportional to the stress invariant J_2, von Mises proposed that the yielding occurs when the deviatoric stress tensor, J_2, exceeds a characteristic value of the material, k. The value of k is found by assuming that yielding begins when the distortional energy due to any stress state equals the distortional energy at yield in simple tension. Mathematically, yielding occurs when

$$J_2 = \frac{\sigma_y}{\sqrt{3}}. \tag{2.11}$$

In other words, yielding is said to occur when the quantity called as the equivalent stress does not exceed the yield stress in a uniaxial tensile test. The equivalent stress σ_e can be expressed as

$$\sigma_e = \frac{1}{\sqrt{2}} \left[(\sigma_1 - \sigma_2)^2 + (\sigma_2 - \sigma_3)^2 + (\sigma_3 - \sigma_1)^2 \right]^{\frac{1}{2}}. \tag{2.12}$$

The Tresca yield criterion assumes that yielding occurs when the maximum shear stress for a multiaxial stress state reaches the maximum shear stress occurring under simple tension. For a given multiaxial stress state, if $\sigma_1 > \sigma_2 > \sigma_3$, the maximum shear stress is

$$\tau_{max} = \frac{\sigma_1 - \sigma_3}{2}. \tag{2.13}$$

The maximum shear stress in a uniaxial tensile test ($\sigma_2 = \sigma_3 = 0$) at yielding is $\frac{\sigma_y}{2}$, which implies that yielding begins when

$$\sigma_1 - \sigma_3 = \sigma_y. \tag{2.14}$$

When plotted on a three dimensional stress space, the Tresca's yield surface is a hexagonal prism inscribed in von Mises's cylindrical surface.

2.4 Plastic Stress-Strain Relationships

The flow rule is the necessary kinematic assumption postulated for plastic flow. It provides the ratio or the relative magnitudes of the components of the plastic strain increment tensor ($d\epsilon_{ij}^p$). The flow rule is developed for the uniaxial case as follows.

15

The hydrostatic or the mean stress for the uniaxial case ($\sigma_1 = \sigma_1, \sigma_2 = 0, \sigma_3 = 0$), is given by

$$\sigma_m = \frac{\sigma_1 + \sigma_2 + \sigma_3}{3} = \frac{\sigma_1}{3}. \tag{2.15}$$

The deviatoric stresses are obtained as

$$\begin{aligned}
\sigma_1' &= \sigma_1 - \sigma_m = \frac{2}{3}\sigma_1 \\
\sigma_2' &= \sigma_2 - \sigma_m = -\frac{1}{3}\sigma_1 \\
\sigma_3' &= \sigma_3 - \sigma_m = -\frac{1}{3}\sigma_1
\end{aligned} \tag{2.16}$$

or

$$\frac{\sigma_1'}{\sigma_2'} = \frac{\sigma_1'}{\sigma_3'} = -2. \tag{2.17}$$

Further, for volume constancy, the sum of plastic strain increments must be zero. Therefore

$$d\epsilon_1 + d\epsilon_2 + d\epsilon_3 = 0. \tag{2.18}$$

Symmetry in the uniaxial case leads to $d\epsilon_2 = d\epsilon_3$ or in other words $d\epsilon_1 = -2d\epsilon_2 = -2d\epsilon_3$, which can be written as

$$\frac{d\epsilon_1}{d\epsilon_2} = \frac{d\epsilon_1}{d\epsilon_3} \approx -2 \tag{2.19}$$

and a comparison with Eq. 2.17 shows that

$$\frac{d\epsilon_1}{\sigma_1'} = \frac{d\epsilon_2}{\sigma_2'} = \frac{d\epsilon_3}{\sigma_3'} = \text{constant} = d\lambda \quad \text{(for a general case).} \tag{2.20}$$

The above equation represents the flow rules postulated for a general case by Prandtl and Reuss [19]. It essentially states that the ratio of current incremental plastic strain increments to the current deviatoric stresses is a constant. The Eq. 2.20 can be manipulated to give the following equations.

$$d\epsilon_1 = \frac{d\bar{\epsilon}}{\bar{\sigma}}\left[\sigma_1 - \frac{1}{2}(\sigma_2 + \sigma_3)\right]$$

16

$$d\epsilon_2 = \frac{d\bar{\epsilon}}{\bar{\sigma}} \left[\sigma_2 - \frac{1}{2} \left(\sigma_3 + \sigma_1 \right) \right]$$
$$d\epsilon_3 = \frac{d\bar{\epsilon}}{\bar{\sigma}} \left[\sigma_3 - \frac{1}{2} \left(\sigma_1 + \sigma_2 \right) \right]. \tag{2.21}$$

The above equation looks similar to the generalized Hooke's law where $\frac{1}{E}$ is replaced by $\frac{d\bar{\epsilon}}{\bar{\sigma}}$ and ν is replaced by $\frac{1}{2}$ as a consequence of incompressibility. The incremental effective strain is given by

$$d\bar{\epsilon} = \frac{\sqrt{2}}{3} \left[(d\epsilon_1 - d\epsilon_2)^2 + (d\epsilon_2 - d\epsilon_2)^2 + (d\epsilon_3 - d\epsilon_2)^2 \right]^{\frac{1}{2}}. \tag{2.22}$$

The coefficient $\frac{\sqrt{2}}{3}$ is so chosen that $d\bar{\epsilon}$ is equal to $d\epsilon_1$ under uniaxial tension.

Due to the nonlinear nature of the plastic constitutive relations, analytical solutions of the boundary-value problems are difficult to obtain. Exact elastic-plastic solutions are available for only few simple problems. In general, a complete load history analysis has to be performed in order to get the solution. Due to the rapid advancement of powerful computers and modern numerical techniques, incremental inelastic analysis of structural problems is carried out by the powerful finite element method.

2.5 Finite Element Formulation

The general governing equation of the finite element method for a static analysis is derived from the principle of virtual work which states that "if a deformable body in equilibrium is subjected to arbitrary virtual displacements associated with a compatible deformation of the body, the virtual work of external forces of the body is equal to the virtual strain energy of the internal stresses". The principle can be expressed as

$$\int_V \sigma_{ij} \delta\epsilon_{ij} \, dV = \int_A T_i \delta u_i \, dA + \int_V q_i \delta u_i \, dV \tag{2.23}$$

17

where δu_i and $\delta \epsilon_{ij}$ are the virtual displacement and virtual strain increments respectively, and form a compatible set of deformations. T_i and q_i are surface traction and body force respectively. For the discretized finite element mesh configuration, Eq. 2.23 is written in matrix form as

$$\int_V \{\delta \epsilon\}^T \{\sigma\} \ dV = \int_A \{\delta u\}^T \{T\} \ dA + \int_V \{\delta u\}^T \{q\} \ dV \qquad (2.24)$$

where the vectors for displacement $\{u\}$, strain $\{\epsilon\}$ and stress $\{\sigma\}$ are given by

$$\{\delta u\}^T = \{\delta u_1, \delta u_2, \delta u_3\}$$
$$\{\delta \epsilon\}^T = \{\delta \epsilon_x, \delta \epsilon_y, \delta \epsilon_z, \delta \gamma_{xy}, \delta \gamma_{xz}, \delta \gamma_{yz}\}$$
$$\{\sigma\}^T = \{\sigma_x, \sigma_y, \sigma_z, \sigma_{xy}, \sigma_{xz}, \sigma_{yz}\}. \qquad (2.25)$$

For a small deformation analysis.

$$\{\delta \epsilon\} = [B] \{\delta U\} \qquad (2.26)$$

where $\{U\}$ is the displacement vector of nodal points that is related to the distributed displacement $\{u\}$ by

$$\{u\} = [N] \{U\} \qquad (2.27)$$

in which $[N]$ is the shape function matrix. The strain displacement matrix $[B]$ and the shape function matrix are related through

$$[B] = [L][N] \qquad (2.28)$$

where $[L]$ is the differential operator matrix. Substituting Eqs. 2.26 and 2.27 in Eq. 2.24, the governing equation for a small deformation analysis in matrix form is obtained as

$$\int_V [B]^T \{\sigma\} \ dV = \int_A [N]^T \{T\} \ dA + \int_V [N]^T \{q\} \ dV \qquad (2.29)$$

or

$$\int_V [B]^T \{\sigma\} \ dV = \{R\} \qquad (2.30)$$

where $\{R\}$ is the equivalent external force acting on the nodal points.

$$\{R\} = \int_A [N]^T \{T\} \, dA + \int_V [N]^T \{q\} \, dV. \tag{2.31}$$

For a linear elastic stress-strain relationship, the governing equation is

$$[K]\{U\} = \{R\} \tag{2.32}$$

where $[K]$ is the stiffness matrix of the structure

$$[K] = \int_V [B]^T [C][B] \, dV \tag{2.33}$$

in which $[C]$ is the elastic constitutive matrix. In the elastic-plastic analysis, because of the non-linear relationship between stress and strain, the governing Eq. 2.23 is a non-linear equation of strains and therefore, a non-linear function of nodal displacements. Iterative methods are used to solve for the displacements for a given set of external loads. The commonly used numerical algorithms are :

1. the tangential stiffness method

2. the initial stiffness method

2.5.1 The Tangential Stiffness Method

If it is assumed that the stresses, strains and displacements at any instant to be represented by σ_0, ϵ_0 and u_0, then the global stiffness matrix K_0 corresponding to this state can be found. K_0 can be considered as the local slope of the force-displacement relationship. If the external loads are increased by ΔF_0 and using the stiffness matrix K_0, the displacements Δu_0, stresses $\Delta \sigma_0$ and strains $\Delta \epsilon_0$ corresponding to this incremental load can be found. Now, the total displacements, stresses and strains are given by $u_0 + \Delta u_0$, $\sigma_0 + \Delta \sigma_0$, $\epsilon_0 + \Delta \epsilon_0$. If the solution has to be improved , another tangential stiffness matrix K_1 can be calculated from the above improved results. For

19

all the elements in which the yield condition is violated ($\phi(\sigma_0 + \Delta\sigma_0) > 0$), the stresses have to be reduced in order to satisfy the yield condition and for plastic deformation to occur. The stress increment $\Delta\sigma_0'$ corresponding to the strain increment $\Delta\epsilon_0$ can be obtained from the elasto-plastic constitutive equation

$$\Delta\sigma_0' = D\Delta\epsilon_0 \tag{2.34}$$

where the matrix D is calculated on the basis of the stresses $\sigma_0 + \Delta\sigma_0$. The residual stress which has to be removed from the element in order to satisfy the yield condition is obtained from the relation

$$\Delta\sigma_0^r = \Delta\sigma_0 - \Delta\sigma_0'. \tag{2.35}$$

The equivalent nodal forces on the elements corresponding to this stress state can be calculated from Eq. 2.30 as

$$\Delta F_0 - \Delta F_0^R = \int B^T \Delta\sigma_0^r \, dA. \tag{2.36}$$

The residual (unbalanced external nodal) forces can now be applied as the next load increment and the procedure is repeated until desired convergence on the displacement is achieved. This iterative procedure is also called the generalized Newton-Raphson method.

2.5.2 The Initial Stiffness Method

In the tangential stiffness method, a new matrix has to be computed every time the load is incremented. This requires more storage space and an increase in computation time. In the initial stiffness method, the stiffness matrix computed from the first iteration is used in subsequent load increments. The solution of the equation $dF = K\,du$ has to be performed only on the first iteration, because the subsequent solutions merely requires the proportional reduction of the solution obtained from the first load
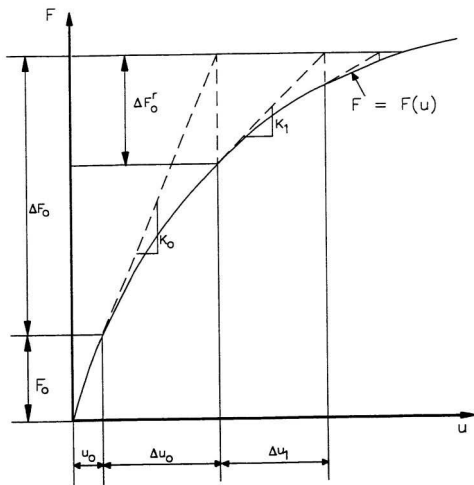
Figure 2.4: Tangential Stiffness Method

step. It can be seen that in the initial stiffness method, the stiffness matrix has to be found only once in the iteration process and is definitely an advantage especially when the model contains large number of nodes. Although, this method reduces the computing time to a fair extent, the rate of convergence is very slow. The most economical method would obviously be the combination of the above two algorithms, where the stiffness matrix is changed only at selected load steps during the iteration process.

2.6 Analysis of Notched Components

Notched engineering components are often subjected to loads that cause localized yielding. The resulting plastic strains are of interest in determining the fatigue life of components using the strain-based approach.

In the elastic range, the notch root stress and the nominal stress are related by a geometric constant k_t, called as the stress concentration factor.

$$\sigma = k_t S \qquad \sigma < \sigma_y. \tag{2.37}$$

In the case of plane stress problems such as thin sheets in tension, the stresses at the notch root can be considered to be uniaxial. Therefore, the expression for strain is given by

$$\epsilon = \frac{k_t S}{E} \tag{2.38}$$

which is valid only in the elastic range. Yielding occurs when the stress at the notch root (Fig. 2.6) reaches yield and occurs at the load

$$P_y = \frac{(b-a)\,t}{k_t}\sigma_y \tag{2.39}$$

and the load corresponding to full plastic yielding is given by

$$P_L = (b-a)\,t\sigma_y. \tag{2.40}$$

22
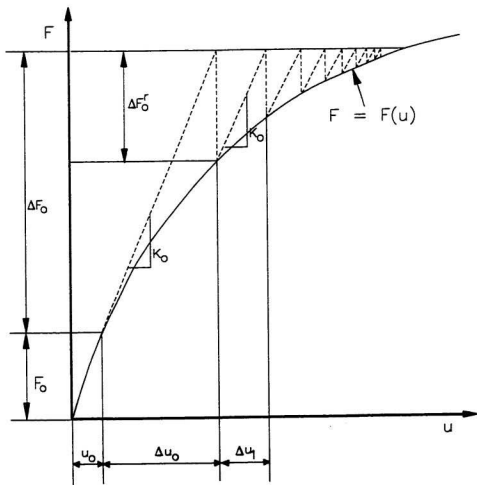
Figure 2.5: Initial Stiffness Method

Only few approximate solutions are available for determining the plastic strains which are important for determining the fatigue life of components. They are:

1. Neuber's rule

2. variations of Neuber's rule proposed by Seeger and Heuler

3. strain energy density method

2.7 Neuber's Rule

Neuber's rule [23] states that during plastic deformation, the geometric mean of stress and strain concentration factors remains invariant and is equal to the elastic stress concentration factor.

If σ_n and ϵ_n are the notch stresses and strains, and S and e are the nominal stresses and strains, then the plastic stress and strain concentration factors are

$$
\begin{aligned}
k_\sigma &= \frac{\sigma_n}{S} \\
k_\epsilon &= \frac{\epsilon_n}{e}
\end{aligned}
\tag{2.41}
$$

and Neuber's rule is given by

$$k_\sigma k_\epsilon = k_t^2. \tag{2.42}$$

If net section yielding does not occur, then the nominal strain can be written as $e = \frac{S}{E}$. Using Eqs. 2.41 and 2.42, we have

$$\sigma_n \epsilon_n = \frac{(k_t S)^2}{E}. \tag{2.43}$$

The above equation can be solved in conjunction with the material stress strain curve in order to obtain the notch stresses and strains. If an elastic-perfectly plastic material is considered, the notch strain can be determined as

$$\epsilon_n = \frac{(k_t S)^2}{\sigma_y E} \tag{2.44}$$

24
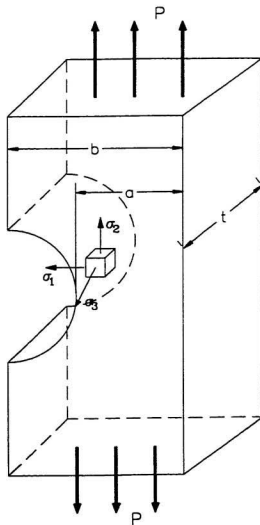
Figure 2.6: Stresses at Notch Root

where σ_y is the yield stress of the material.

The above rule does not account for general yielding effects. Further, general yielding may not occur when S equals σ_y as in the case of bending. In order to account for the non-linear net section behavior, Seeger and Heuler [28], proposed a modified version of Neuber's Rule which can also be used for combined loading cases. The relation is expressed as

$$\sigma\epsilon = k_p^2 S^* \epsilon^* \tag{2.45}$$

where k_p is the plastic limit load factor and is given by

$$k_p = \frac{S \text{ at onset of general yielding}}{S \text{ at first notch yielding}} = \frac{S_p}{\frac{\sigma_y}{k_t}} \tag{2.46}$$

where k_t and S are defined in consistent manner, either net or gross section. S_p is a particular value of S corresponding to fully plastic behavior for an elastic-perfectly plastic material having the same yield strength as the material under consideration. If the material stress strain curve is assumed to be elastic-perfectly plastic, then k_p equals k_t.

2.8 Extension to Plane Strain Problems

In the case of axisymmetric sections such at shafts and notched cylinders, when the notch radius ρ is small compared with the other dimensions of the shafts, the situation at the vicinity of the notch approaches the plane strain condition. Under this condition, σ_1 is zero due to the free surface (Fig. 2.6). Since $\epsilon_3 = 0$ due to the plane strain assumption, a situation of plane stress exists in the 2-3 plane, and the stresses in the 2 and 3 direction are related by

$$\sigma_3 = \bar{\nu}\sigma_2 \tag{2.47}$$

26

where

$$\bar{\nu} = \frac{\nu + \dfrac{0.5 E \bar{\epsilon}_p}{\bar{\sigma}}}{1 + \dfrac{E \bar{\epsilon}_p}{\bar{\sigma}}}. \tag{2.48}$$

The quantity $\bar{\nu}$ reduces to the elastic Poisson's ratio if there are no plastic strains and increases to 0.5 when the plastic strains are large [10]. Using the Eq. 2.47 and 2.48, the uniaxial stress-strain curve can be modified for the plane strain condition as

$$\begin{aligned} \sigma'_2 &= \frac{\sigma_e}{\sqrt{1 - \bar{\nu} - \bar{\nu}^2}} \\ \epsilon'_2 &= \frac{\epsilon_{eqv}\,(1 - \bar{\nu}^2)}{\sqrt{1 - \bar{\nu} - \bar{\nu}^2}}. \end{aligned} \tag{2.49}$$

This stress-strain curve can be used in conjunction with Neuber's rule to obtain the strains at the notch root.

2.9 Molski-Glinka Method

Molski and Glinka [20] proposed a method to calculate the notch root stresses and strains based on strain energy considerations. In the elastic regime, the strain energy per unit volume due to the local stress σ is given by

$$W_\sigma = \frac{\sigma^2}{2E} \tag{2.50}$$

and the elastic strain energy per unit volume due to the nominal remote stress S is

$$W_S = \frac{S^2}{2E}. \tag{2.51}$$

The stress concentration factor k_t in the elastic region can be obtained as

$$k_t = \frac{\sigma}{S} = \left(\frac{W_\sigma}{W_S}\right)^{0.5}. \tag{2.52}$$

When the stress at the notch root increases beyond the yield, plastic deformation occurs. It is assumed that the energy ratio does not change due the small plastic

27

region. The relatively high volume of the elastic material surrounding the small plastic zone controls the amount of strain energy absorbed by the plastic zone. Thus, the ratio of strain energy is assumed constant even during the plastic deformation. However, the material stress-strain relationship is used to determine the strain energy absorbed by the notch root. If a Ramberg-Osgood relation of the form

$$\epsilon = \epsilon_e - \epsilon_p = \frac{\sigma}{E} - \left(\frac{\sigma}{K}\right)^{\frac{1}{n}} \qquad (2.53)$$

is used, where n is the strain hardening exponent and K is the strength coefficient, then, Eq. 2.52 can be modified to give

$$\frac{(k_t S)^2}{2E} = \frac{\sigma^2}{2E} - \frac{\sigma}{n'-1}\left(\frac{\sigma}{K'}\right)^{\frac{1}{n'}} \qquad (2.54)$$

Eqs. 2.53 and 2.54 can be used simultaneously to obtain the notch root stress σ and strain ϵ respectively.

The energy interpretation of Neuber's Rule and the strain energy density method is shown in Fig. 2.7. OABC is the strain energy due to the nominal stresses. OADE is the strain energy absorbed by the MG method and OAFG is the strain energy absorbed by Neuber's rule.

2.10 Multiaxial Elasto-Plastic Notch Root Stress-Strains

Hoffman and Seeger [13] proposed a method to obtain complete information on the multiaxial elastic-plastic stress and strain states at the notch root. Recently, Glinka et al. [21] have extended the energy density method to multiaxial stress states. The complete solution in both the methods essentially consists of three steps.

- In the the method proposed by Hoffman and Seeger, Neuber's rule is used in its equivalent form to relate the equivalent stresses and strains. The pseudo elastic

28
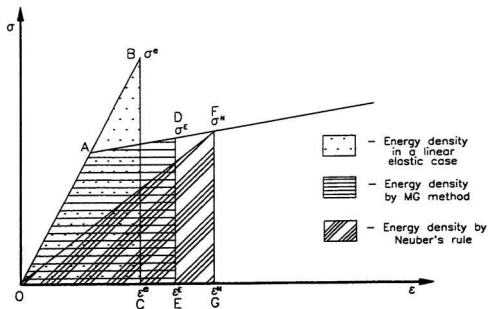
Figure 2.7: Energy interpretation of Glinka and Neuber Methods

quantities can be written in the form

$$\epsilon_{equ} = \frac{K_{te}^2 S^2}{\sigma_e E} \qquad (2.55)$$

where K_{te} is the equivalent stress concentration factor. In order to obtain the strain in the non-linear nominal stress range, the plastic limit load factor has to be known.

In the energy density method, the notch root strain energies are related to the nominal strain energies. For an arbitrary multiaxial state on the principal axes, the strain energy relation leads to

$$\int \left(\sigma_1^e d\epsilon_1^e + \sigma_2^e d\epsilon_2^e + \sigma_3^e d\epsilon_3^e \right) = \int \left(\sigma_1^E d\epsilon_1^E + \sigma_2^E d\epsilon_2^E + \sigma_3^E d\epsilon_3^E \right). \qquad (2.56)$$

• In both the methods, Hencky's rule is used to relate the stresses and strains in the plastic regime which assumes the plastic strains to be a function of deviatoric stresses.

$$\epsilon_i^p = \frac{3}{2} \frac{\epsilon_{equ}^p}{\sigma_e} \sigma_i', \qquad i = 1, 2, 3. \qquad (2.57)$$

It is assumed that the deviatoric stress components (at the notch tip) do not change much (at the notch tip) and that no unloading occurs.

• One of the stresses normal to the notch surface would be zero due to the free surface. Therefore, it is necessary to make one assumption in order to solve for all the stress and strain components.

Hoffman and Seeger have assumed in the elastic-plastic region a constant ratio of $\frac{\epsilon_2}{\epsilon_1}$ equal to the ratio in the elastic region.

In the energy density method, it is assumed that the ratio of the largest notch tip principal strain energy to the notch tip total strain energy is equal to the

corresponding ratio which is calculated for a geometrically identical linear elastic body.

$$\frac{\sigma_2^A \epsilon_2^A}{\sigma_{ij}^A \epsilon_{ij}^A} = \frac{\sigma_2^E \epsilon_2^E}{\sigma_{ij}^E \epsilon_{ij}^E}. \tag{2.58}$$

The above set of equations can be solved for determining the elastic-plastic stresses and strains at the notch root.

2.11   Fatigue

Accumulation of damage due to cyclic loading and subsequent failure is called fatigue. The two types of fatigue failures produced by different physical mechanisms are :

- High Cycle Fatigue

- Low Cycle Fatigue

Failures associated with lower loads and long lives or high number of cycles to produce fatigue failure is commonly referred to as high cycle fatigue. In this case, strains cycles are mostly confined to the elastic range. Failures associated with high loads and short lives or low number of cycles to produce fatigue failure is referred to as low cycle fatigue. Plastic deformation may occur in localized regions, such as stress raisers, where fatigue cracks are likely to begin. Low cycle fatigue is associated with cycle lives up to 10^4 cycles and high cycle fatigue for lives greater than 10^4 cycles.

The stress-strain response of most materials change significantly with cyclic strains initially, but the hysteresis loop tends to stabilize so that the stress amplitude remains constant in strain control over the remaining portion of the fatigue life. Hysteresis loops from near half the fatigue life are conventionally used to represent the approximately stable behavior. A line joining the origin and the tip of the loops is the cyclic

31

stress-strain curve (Fig. 2.8) which is the relationship between stress and strain for cyclic loading.

Since plastic strains are the controlling variable in the low cycle fatigue regime. Mason and Coffin [6] proposed an empirical relation

$$\frac{\Delta\epsilon}{2} = \epsilon'_f \left(2N_f\right)^c \tag{2.59}$$

where

$$\frac{\Delta\epsilon}{2} = \text{plastic strain amplitude}$$

$$\epsilon'_f = \text{fatigue ductility coefficient}$$

$$2N_f = \text{total reversals to failure}$$

$$c = \text{fatigue ductlity exponent.}$$

The quantities ϵ'_f and c are material constants.

The strain based approach can also be applied where there is little plasticity at long lives, making it as a comprehensive one that can be used in place of stress based approach. Morrow et al. [6] used total strain amplitude in place of plastic strain amplitude.

$$\frac{\Delta\epsilon}{2} = \frac{\sigma'_f}{E}\left(2N_f\right)^b + \epsilon'_f\left(2N_f\right)^c \tag{2.60}$$

where the material constants b and c are the slopes of elastic and plastic curves and the constants $\frac{\sigma'_f}{E}$ and ϵ'_f are one reversal intercepts (i.e. $2N_f = 1$) of elastic and plastic curves respectively.

A tensile mean stress was found to give shorter fatigue lives and compressive mean stress, longer fatigue lives than a zero mean stress. Morrow modified Eq. 2.60 to account for the non-zero mean stress effects and proposed the following relation

$$\frac{\Delta\epsilon}{2} = \frac{\sigma'_f}{E}\left(1 - \frac{\sigma_m}{\sigma'_f}\right)\left(2N_f\right)^b + \epsilon'_f\left(1 - \frac{\sigma_m}{\sigma'_f}\right)^{\frac{c}{b}}\left(2N_f\right)^c. \tag{2.61}$$

32
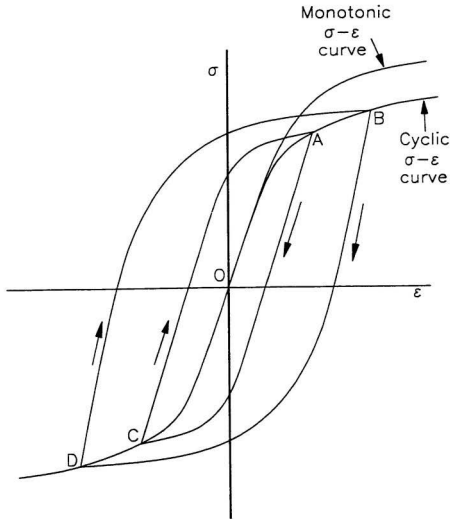
Figure 2.8: Monotonic and Cyclic Stress-Strain Curves

In the above equation, the material constants $\sigma'_f, \epsilon'_f, c$ and b can be obtained from literature [4]. The strain amplitude $\Delta\epsilon$, can be determined from inelastic finite element analysis. Neuber's rule or the GLOSS method, later described in this thesis, which gives good estimate of inelastic strain from only two linear elastic finite element analysis.

Chapter 3

The GLOSS Method

3.1 Uniaxial and Multiaxial Relaxation

Uniaxial stress relaxation data are obtained by subjecting a uniaxial member to a fixed strain and measuring the reduction in the initial stress as a function of time. The situation wherein the initial strain is held fixed is referred to as deformation controlled. Since the strain is held constant, the stress-strain response for such a case is depicted by the line AB (Fig. 3.1). On the other hand if an axial load is applied to the uniaxial member, internal stresses are set up to balance the external load that does not change with time. Such a response is termed as load controlled and on the stress-strain plot, the response is depicted by the line AC. In general, however, the response is neither load controlled nor deformation controlled, and this mixed-mode response is termed as follow-up and is depicted by the line AD.

More often than not stresses in a given mechanical component are multiaxial. On an intuitive basis, Seshadri and Mikulcik [36] recognized that the effect of multiaxiality is to speed up or slow down the uniaxial relaxation process. Consequently, uniaxial and multiaxial relaxation can be related as $\tau_{mult} = \frac{\tau_{uniaxial}}{\bar{\lambda}}$ and $\bar{\lambda}$ is designated as the constraint parameter by Seshadri and Mikulcik. The constraint parameter essentially characterizes the interaction between the local region and the remainder region. If the local plastic zone is very small then the predominantly elastic remainder region
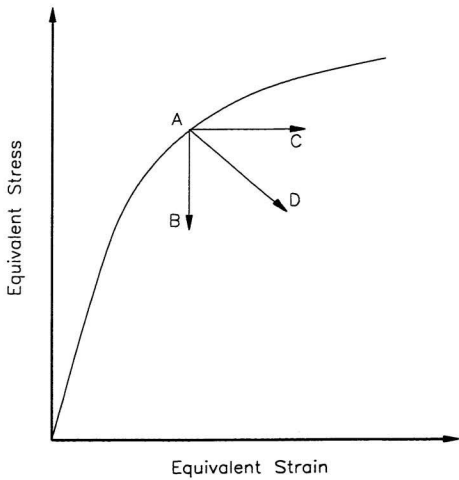
Figure 3.1: Load control, deformation control and follow-up

controls the local region response leading to a deformation-controlled behavior of the local element. When the plastic zone spreads across the entire cross section, the structure or component becomes statically determinate leading to load-control behavior. When the plastic zone is in between, the local element will exhibit follow-up behavior.

For a uniaxial member subjected to a fixed strain, the sum of elastic, plastic and creep strain rate components at any time can be expressed as

$$\dot{\epsilon}_t(t) = \dot{\epsilon}_{el}(t) + \dot{\epsilon}_{pl}(t) + \dot{\epsilon}_{cr}(t). \tag{3.1}$$

In the above equation, the elastic strain rate is $\dot{\epsilon}_{el} = \left(\dfrac{1}{E}\right)\left(\dfrac{d\sigma}{dt}\right)$, the plastic strain rate is equal to zero, the creep strain rate is $\dot{\epsilon}_{cr} = B\sigma^n$ and the total strain is $\dot{\epsilon}_t = 0$. Eq. 3.1 can therefore be written as

$$\frac{d\sigma}{dt} + BE\sigma^n = 0. \tag{3.2}$$

The solution for the above equation can be expressed as

$$\sigma(t) = \left[\frac{1}{\sigma_i^{n-1}} + BE(n-1)t\right]^{\frac{-1}{(n-1)}}. \tag{3.3}$$

Since multiaxial relaxation and uniaxial relaxation are related by the constraint parameter, $\tau_{uniaxial} = \tau_{mult}\bar{\lambda}$, Eq. 3.2 simply gets modified as

$$\frac{d\sigma_e}{d\tau} + \bar{\lambda}BE\sigma_e^n = 0 \tag{3.4}$$

and the solution can be written as

$$\sigma_e(t) = \left[\frac{1}{\sigma_i^{n-1}} + \bar{\lambda}BE(n-1)\tau\right]^{\frac{1}{(1-n)}}. \tag{3.5}$$

Therefore, when $\bar{\lambda}$ is known, the stress relaxation for multiaxial constraints can be determined using the above expression. As well, when $\bar{\lambda} = 1$ the situation becomes a uniaxial case of deformation controlled. When $\bar{\lambda} = 0$, the stresses do not relax as it corresponds to a load controlled situation.

3.2 Determination of Multiaxial Constraint Parameter

Kizhatil and Seshadri [16] have developed a generalized relation for the determination of $\bar{\lambda}$ involving the principal stress and strain ratios. For a structure undergoing creep with a uniaxial creep relationship of the form $\dot{\epsilon}_{cr} = \psi\,(\sigma,\tau)$, the stress relaxation for a multiaxial case is given by

$$\frac{d\sigma_e}{d\tau} + \bar{\lambda}\,(\tau)\,\psi E = 0 \tag{3.6}$$

where

$$\bar{\lambda} = \frac{f\,(\alpha_1, \alpha_2, \alpha_3, \beta_1, \beta_2, \beta_3)}{g\,(\alpha_1, \alpha_2, \alpha_3)} \tag{3.7}$$

and f and g are given by

$$\begin{aligned}
f &= \left[\alpha_1 - \frac{1}{2}\,(\alpha_1 + \alpha_2) - \beta_1\right]\left[\alpha_1\,(2 - 4\nu) + (\alpha_2 + \alpha_3)\,(2\nu - 1)\right] \\
&+ \left[\alpha_2 - \frac{1}{2}\,(\alpha_3 + \alpha_1) - \beta_2\right]\left[\alpha_2\,(2 - 4\nu) + (\alpha_3 + \alpha_1)\,(2\nu - 1)\right] \\
&+ \left[\alpha_3 - \frac{1}{2}\,(\alpha_1 + \alpha_2) - \beta_3\right]\left[\alpha_3\,(2 - 4\nu) + (\alpha_1 + \alpha_2)\,(2\nu - 1)\right] \\
g &= \left(1 - \nu - 2\nu^2\right)\left[(\alpha_1 - \alpha_2)^2 + (\alpha_2 - \alpha_3)^2 + (\alpha_3 - \alpha_1)^2\right]
\end{aligned} \tag{3.8}$$

where $\alpha_1 = \frac{\sigma_1\,(\tau)}{\sigma_1\,(\tau)}$, $\alpha_2 = \frac{\sigma_2\,(\tau)}{\sigma_1\,(\tau)}$, $\alpha_3 = \frac{\sigma_3\,(\tau)}{\sigma_1\,(\tau)}$. $\beta_1\,(\tau) = \frac{\dot{\epsilon}_{t1}}{(\psi/\sigma_e)\,\sigma_1}$ $\beta_2\,(\tau) = \frac{\dot{\epsilon}_{t2}}{(\psi/\sigma_e)\,\sigma_1}$ and $\beta_3\,(\tau) = \frac{\dot{\epsilon}_{t3}}{(\psi/\sigma_e)\,\sigma_1}$. The above equation for $\bar{\lambda}$ is expressed in terms of the stress ratios and the time-dependent strain rates. As a first approximation, the stress ratios can be considered to be constant, which is generally valid during the early part of the relaxation cycle where most of the creep-damage in pressure components is likely to occur. The expression can be then specialized for two dimensional constraints where the total strains are held fixed in two directions, and three dimensional constraints where the total strains are held fixed in all the directions.

The determination of $\bar{\lambda}$ for a general mechanical component configuration from the above expressions requires the knowledge of principal stress and strain ratios.

The GLOSS (Generalized Local Stress Strain) analysis is a more direct method for determining the constraint parameter on the basis of two linear elastic finite element analyses. The method can be applied to any component configuration of practical relevance.

3.3 The GLOSS Method

The component under consideration is divided into local and remainder regions. The local region experiences inelastic effects and is the region of interest from the design standpoint. The GLOSS theory relates the multiaxial stress distribution in the local region to the uniaxial redistribution process. The local region quantities are designated by superscript 'o', while the remainder region quantities are designated by superscript 'r'. The multiaxial stresses and strains are idealized as uniaxial case and are shown in the Fig. 3.2. The strain distribution can be expressed as

$$\dot{\epsilon}_{el} + \bar{\lambda}\dot{\epsilon}_{cr} = 0 \qquad (3.9)$$

where $\bar{\lambda}$ is the constraint parameter which characterizes the interaction between the local and the remainder regions. Since the total local strain $\dot{\epsilon}_t$ is the sum of elastic, plastic and creep strains, and given that the plastic strains do not vary with time, $\dot{\epsilon}_p = 0$. Therefore

$$\dot{\epsilon}_t = \dot{\epsilon}_{el} + \dot{\epsilon}_c. \qquad (3.10)$$

Combining Eqs. 3.9 and 3.10

$$\dot{\epsilon}_{el} = \left(\frac{\bar{\lambda}}{\bar{\lambda} - 1}\right)\dot{\epsilon}_t. \qquad (3.11)$$

Since $\dot{\epsilon}_{el} = \dfrac{1}{E_o}\dfrac{d\sigma_e}{d\tau}$, the relaxation modulus E_r can be defined as

$$E_r = \frac{d\sigma_e}{d\tau} = \frac{1}{\dot{\epsilon}_t}\left(\frac{d\sigma_e}{d\tau}\right) = \left(\frac{\bar{\lambda}}{\bar{\lambda} - 1}\right)E_o. \qquad (3.12)$$
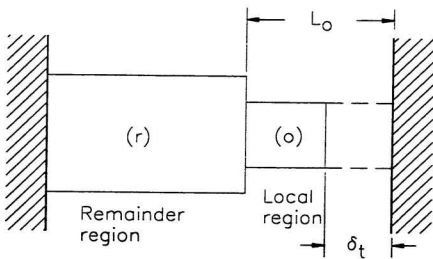
Figure 3.2: One dimensional relaxation model

Normalizing the relaxation modulus such that $\bar{E}_r = \frac{E}{E_o}$. the above equation can be expressed in term of $\bar{\lambda}$ as

$$\bar{\lambda} = \frac{\bar{E}_r}{\bar{E}_r - 1}. \tag{3.13}$$

Once the relaxation modulus E_r is known, the constraint parameter can be determined.

3.4 Relaxation Modulus, E_r

The GLOSS diagram (Fig. 3.3) is a plot of normalized equivalent stress versus the normalized total equivalent strain that is generated on the basis of two linear elastic finite element analysis. A first finite element analysis is carried out assuming the material behavior to be completely linear elastic. The equivalent stress and strain of the highest stressed element is identified as the local region and the quantities are denoted as σ_{e1} and ϵ_{e1}. The elastic modulii of all the elements above nominal yield are identified and modified according to the expression

$$E_s = \frac{\sigma_y}{\sigma_{ei}} E_o \tag{3.14}$$

where σ_{ei} is the von Mises equivalent stress of the ith element.

A second linear elastic finite element analysis is carried out next after making the above modification. The stress and strain of the local element is determined as σ_{e2} and ϵ_{e2}. On the basis of the two linear elastic finite element analysis, the GLOSS diagram can be constructed.

OAC is the elastic perfectly plastic stress strain curve and OD is the elastic line. The pseudo elastic point D($\sigma_{e1}, \epsilon_{e1}$), of the local element is located on this elastic line. The stress and strain of the local element ($\sigma_{e2}, \epsilon_{e2}$) determined from the second linear elastic finite element is represented by point E. The slope of the line OE is called as

41

Figure 3.3: GLOSS Diagram

the secant modulus and that of the DE is the relaxation modulus. The relaxation modulus is given by

$$E_r = \frac{\sigma_{e1} - \sigma_{e2}}{(\epsilon_{e2} - \epsilon_{e1})E_o} \tag{3.15}$$

from which $\bar{\lambda}$ can be determined. It was shown earlier that the constraint parameter $\bar{\lambda}$ was a function of principal stress and strain ratios which can vary with time. Consequently, E_r is also a function of principal stresses and strains which vary with time. It was also pointed out that the principal stresses and strains were reasonably constant during the early portion of relaxation and. as a first approximation. $\bar{\lambda}$ can be treated as a constant during this initial part of relaxation. For small to moderate amounts of follow-up, the constraint parameter and the relaxation modulus do not vary with time irrespective of whether the inelastic response of the structure is due to steady-state creep or time independent plasticity. GLOSS analysis can therefore be used to determine the inelastic effects due to plasticity as well as creep. Thus the line DE can be extended to intersect the material stress strain curve. The local region inelastic strain can therefore be determined.

The angle θ is the measure of the degree of multiaxiality and follow-up present in the local element. When θ equals 0 and the stresses relax with strains remaining constant, pure deformation-control action is said to occur. When θ equals 90° load control action occurs. For cases where there is significant amount of follow-up one more analysis can be performed in order to get an improved estimate of inelastic strain.

3.5   GLOSS with Plasticity Correction

In the case of notched configurations, the nominal plastic zone established from the first linear elastic analysis is smaller than the actual plastic zone. From Fig. 3.4, it can be seen that the plastic zone under contour Γ_1 is the nominal plastic zone

whereas the region under contour Γ_2 is the actual plastic zone. The elements with the region Γ_2 need to be modified in order to obtain good estimate of inelastic strain. A method was proposed by Seshadri and Kizhatil [34] to establish a more realistic plastic zone size in a manner similar to Irwin's crack tip plastic zone correction in fracture mechanics.

From Fig. 3.4. it can be seen that the excess force is due to the area S_1. With respect to the finite element discretization, the excess force can be computed as

$$F_{unbalance} = \sum_{k=1}^{N} (\sigma_e - \sigma_y) A_k \qquad (3.16)$$

where N is the total number of elements under the region S_1, A_k is the area of the typical element considered and σ_e is the equivalent stress of the element determined from the first linear elastic analysis. This excess force has to be accounted for in order to establish the exact plastic zone size. This can be accomplished by the lowering the yield stress to the value σ_y', so that the excess force can be accounted for by equating

$$(\sigma_e - \sigma_y) A_k = \left(\sigma_y - \sigma_y'\right) A_k. \qquad (3.17)$$

Thus, the modified yield can be found as

$$\sigma_y' = 2\sigma_y - \sigma_e. \qquad (3.18)$$

The modified secant modulus is now given by

$$E_s' = \left(\frac{\sigma_y'}{\sigma_e}\right) E_o = \left[2\frac{\sigma_y}{\sigma_e} - 1\right] E_o. \qquad (3.19)$$

The stress distribution adjacent to the notch obtained from the first and the second linear elastic finite element analysis using the above modification is shown in Fig. 3.4. The area under the curve I is given by

$$S_a = S_1 + S_2 + S_5 + S_6. \qquad (3.20)$$
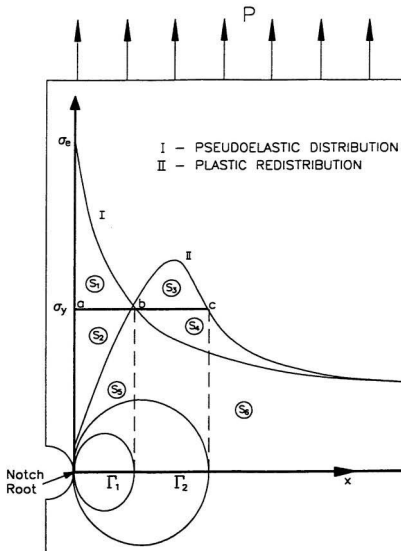
Figure 3.4: Stress at the ahead of notch tip

The area under the curve II is given by

$$S_J = S_3 + S_4 + S_5 + S_6. \tag{3.21}$$

Since both stress distributions are statically admissible, both areas are equal implying that

$$S_\alpha = S_J \tag{3.22}$$

or

$$S_1 + S_2 = S_3 + S_4. \tag{3.23}$$

By the modified softening process, described by the Eq. 3.19

$$S_1 + S_2 = 0. \tag{3.24}$$

This establishes the nominal yield zone denoted by the line ab. Therefore, from Eq. 3.23, $S_3 + S_4 = 0$ implying that the actual yield zone is denoted by the line abc.

In actual components curves I and II do not intersect exactly at point b because of varying amounts of follow-up. The strain estimates obtained by the above method have found be better than the estimate obtained by the GLOSS method explained in the previous section.

Chapter 4

Multibar Models

4.1 Two-Bar Model

In this chapter, the GLOSS method is explained using a two-bar model (Fig. 4.1). The two-bar system is subjected to combined mechanical and thermal loadings. The bar stresses and strains are determined by invoking the equilibrium, strain-displacement and stress-strain relationships as follows:

- Equilibrium Equation :

$$\sigma_1 A_1 + \sigma_2 A_2 = P \tag{4.1}$$

- Strain-Displacement Equation :

$$\epsilon_{t1} = \epsilon_{1e} + \epsilon_{1\theta} = \frac{\delta_1}{L_1}$$
$$\epsilon_{t2} = \epsilon_{2e} + \epsilon_{2\theta} = \frac{\delta_2}{L_2} \tag{4.2}$$

- Stress-Strain Relationship :

$$\epsilon_{1e} = \frac{\sigma_1}{E_1}$$
$$\epsilon_{2e} = \frac{\sigma_2}{E_2} \tag{4.3}$$

For the two bar model the thermal strains are
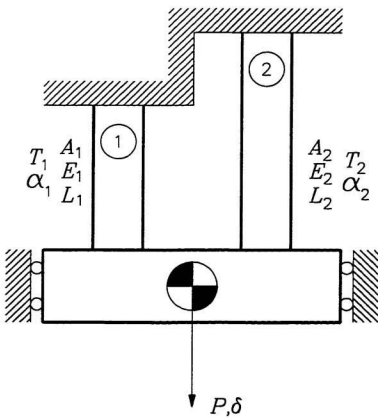
$$\epsilon_{1\theta} = \alpha_1 \Delta T_1$$
$$\epsilon_{2\theta} = \alpha_2 \Delta T_2. \tag{4.4}$$

Figure 4.1: Two-Bar Model

On the basis of Eqs. 4.2, 4.3 and 4.4, the expressions for the total component strains can be obtained as

$$\epsilon_{t1} = \frac{\sigma_1}{E_1} + \alpha_1 \Delta T_1.$$
$$\epsilon_{t2} = \frac{\sigma_2}{E_2} + \alpha_2 \Delta T_2. \tag{4.5}$$

Compatibility of deformations requires that $\delta_1 = \delta_2 = \delta$. Therefore

$$\delta = \epsilon_{t1} L_1 = \epsilon_{t2} L_2. \tag{4.6}$$

Combining Eqs. 4.1, 4.2 and 4.6, the bar stresses can be obtained as

$$\sigma_1 = \frac{\dfrac{P}{E_2 A_2} + \alpha_2 \Delta T_2 - \dfrac{L_1}{L_2} \alpha_1 \Delta T_1}{\dfrac{1}{E_1} \dfrac{L_1}{L_2} + \dfrac{1}{E_2} \dfrac{A_1}{A_2}} \tag{4.7}$$

$$\sigma_2 = \frac{P}{A_2} - \frac{A_1}{A_2} \sigma_1. \tag{4.8}$$

If the material and geometric parameters are so chosen, such that σ_1 is greater than σ_2, then bar 1 is considered as the local bar. The relaxation of bar 1 can be studied by softening the modulus of elasticity of bar 1. The relaxation of bar 1 is studied by setting $E_1' = \gamma E_1$. Eqs. 4.1 - 4.6 are used to solve for the stresses, with ϵ_{1e} now being equal to $\dfrac{\sigma_1'}{\gamma E_1}$. The stresses for the relaxed system are given by

$$\sigma_1' = \frac{\dfrac{P}{E_2 A_2} + \alpha_2 \Delta T_2 - \dfrac{L_1}{L_2} \alpha_1 \Delta T_1}{\dfrac{1}{\gamma E_1} \dfrac{L_1}{L_2} + \dfrac{1}{E_2} \dfrac{A_1}{A_2}} \tag{4.9}$$

$$\epsilon_{t1}' = \frac{\sigma_1}{\gamma E_1} + \alpha_1 T_1. \tag{4.10}$$

The relaxation modulus E_r is given by

$$E_r = \frac{d\sigma}{d\epsilon_t} = \frac{\sigma_1 - \sigma_1'}{\epsilon_{t1} - \epsilon_{t2}}. \tag{4.11}$$

Substituting Eqs. 4.7 and 4.9 into 4.11, and carrying out the necessary simplifications, the following expression can be obtained

$$\bar{E}_r = \frac{E_r}{E_1} = -\frac{A_2 E_2 L_1}{A_1 E_1 L_2}. \tag{4.12}$$

It can be seen that when $\frac{A_2}{A_1} \to \infty$, $\bar{E}_r \to \infty$ signifying deformation control, while $\bar{E}_r \to 0$ when $\frac{A_2}{A_1} \to 0$ signifying load control. All other finite values of $\frac{A_1}{A_2}$ represent various amounts of follow-up.

The constraint parameter can be obtained using Eq. 3.13 as

$$\bar{\lambda} = \frac{L_1}{L_1 + L_2}. \tag{4.13}$$

It can be seen that the constraint parameter is independent of γ, the amount of softening of the local system elastic modulus. This is attributed to the fact that the remainder system (bar 2) drives the local system quite independently of the local system material behavior.

4.2 Analytical Expression for Local Bar Inelastic Strains

Fig. 4.2 shows the GLOSS diagram for the two-bar model. The GLOSS plot is a normalized plot of local bar total axial stress and strain. Point A is the local bar stress and strain corresponding to the first linear elastic analysis. When the local bar is softened, the local bar stress relaxes and is denoted by the point B. Assuming the relaxation locus to be linear, the local bar inelastic strain is predicted by the point C.

From similar triangles ADB and AEC, the local inelastic strain ϵ_{ty} is given by

$$\epsilon_{ty} = \frac{\epsilon_{t1} - \epsilon_{t1}'}{\sigma_1 - \sigma_1'}(\sigma_1 - \sigma_y) + \epsilon_1 \qquad (4.14)$$

where σ_y is the yield strength of the elastic-perfectly plastic material. Expressing the above equation in terms of stresses, we have

$$\epsilon_{ty} = \frac{\frac{\sigma_1'}{\gamma E} - \frac{\sigma_1}{E}}{\sigma_1 - \sigma_1'}(\sigma_1 - \sigma_y) + \frac{\sigma_1}{E} + \alpha_1 \Delta T_1. \qquad (4.15)$$

Substituting the stress from Eqs. 4.7 and 4.9 into the above equation, the local bar strain is given by

$$\epsilon_{ty} = \frac{PL_2 - \sigma_y A_1 L_2 + E_2 A_2 L_2 \alpha_2 T_2}{E_2 A_2 L_1}. \qquad (4.16)$$

The inelastic strain can be found analytically for this simple two-bar model. The material is assumed to be elastic-perfectly plastic. Once the stress in bar 1 reaches yield, the stress remains at σ_y. Now, from the equilibrium equation (4.1), σ_2 can be obtained as

$$\sigma_2 = \frac{P - \sigma_y A_1}{A_2}. \qquad (4.17)$$

Compatibility equation lead to the expression

$$\epsilon_{ty} = \epsilon_2 \frac{L_2}{L_1} = \left(\frac{\sigma_2}{E_2} + \alpha_2 \Delta T_2\right)\frac{L_2}{L_1}. \qquad (4.18)$$

Combining Eqs. 4.17 and 4.18, the local bar total strain can be written as

$$\epsilon_{ty} = \frac{PL_2 - \sigma_y A_1 L_2 + E_2 A_2 L_2 \alpha_2 T_2}{E_2 A_2 L_1}. \qquad (4.19)$$

Therefore, from Eqs. 4.16 and 4.19, it can be seen that the total strain in the local bar predicted by both the modulus reduction method and analytical methods are same.

4.3 Finite Element Modeling and Results

The two-bar is modeled in ANSYS finite element software. The bars are modeled as link elements capable of taking axial compressive and tensile stresses. They are
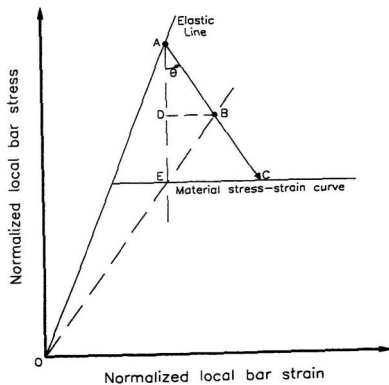
Figure 4.2: GLOSS Diagram for Two-bar Model

52

fixed at one end and coupled at the other end in order to simulate the rigid bar condition.

- Dimensions of the two-bar model :

  Length of bar 1 = 1 in.

  Length of bar 2 = 5 in.

  Area of cross-section of bar 1 = 0.01 in^2

  Area of cross-section of bar 2 = 0.1 in^2

- Material properties :

  Modulus of elasticity, E = 2×10^5 psi

  Yield stress, σ_y = 400 psi

  Coefficient of Thermal Expansion for both bars = 2×10^{-5} per $^\circ C$

The model is subjected to different combination of mechanical and thermal load and the results are reported in Table 4.1. It can be seen from the table that the strain predictions are the same as the results obtained from inelastic finite element analysis.

Table 4.1: Comparison of GLOSS and Inelastic strain estimates

P	$\Delta T1$	$\Delta T2$	Local Bar Strain	
(lb)	($^\circ C$)	($^\circ C$)	GLOSS	Inelastic FEA
20	0	0	0.004	0.004
0	40	40	0.0022	0.0022
20	40	40	0.0072	0.0072
0	50	45	0.0025	0.0025
20	20	10	0.0046	0.0046

Chapter 5

Relaxation Locus

5.1 Introduction

In Chapter 3, both the GLOSS method and the GLOSS method with Plasticity Correction were shown to be robust techniques that are capable of predicting local region inelastic strains on the basis of two linear elastic finite element analyses. In both methods, the stress relaxation locus was implied to be linear as a first approximation. A closer study of the relaxation locus would be useful in verifying the assumption of its linearity.

In addition to evaluating the local strain, the complete relaxation locus also enables the determination of the primary stress or the so-called reference stress of the component. The determination of reference stress is useful since it has extensive application in the integrity assessment of mechanical components and structures as described in Nuclear Electric's R5 and R6 documents [24, 25]. These assessments include low-cycle fatigue, elastic-plastic fracture, creep damage, creep-crack growth and stress classification.

5.2 Reference Stress

The reference stress method developed in U. K. during 1960's, was primarily used to correlate creep deformations in a structure with the results of an equivalent simple

creep test, that is performed at the reference stress σ_R [17]. The reference stress was found to be independent of the creep exponent. Since the solution of a infinite creep exponent is analogous to the limit solution corresponding to perfect plasticity, Sim [38] proposed that the reference stress can be obtained from the relationship

$$\sigma_R = \frac{P}{P_L}\sigma_y \tag{5.1}$$

where P is the load on the structure, P_L is the limit load and σ_y is the yield stress.

In 1991. Seshadri [29] introduced the concept of r-nodes in order to determine the limit loads of mechanical components and structures using two linear elastic finite element analyses. Similar to the GLOSS method, the inelastic stress redistribution is simulated by modifying the elastic modulii of all the elements in the structure. In certain locations of the structure the stresses do not change during stress redistribution. These locations were called redistribution nodes or r-nodes. The r-nodes were identified as load-controlled locations that are induced in order to preserve equilibrium with externally applied forces and moments. The insensitivity to the inelastic constitutive relationship exhibited by the r-node stresses and reference stress was established. The reference stress was identified as primary stress and was unified with the stress-classification concepts (as described in ASME Codes) in a paper by Seshadri and Marriott [35].

When widespread inelastic action such as plasticity or creep occurs, the statically indeterminate stresses undergo a redistribution throughout the component. Since the r-nodes are locations within a component or a structure that are statically determinate, for fixed external loads the stresses do not change at these locations during the inelastic stress redistribution process. The r-nodes stresses are therefore insensitive to the inelastic constitutive relationship of the component material, and are, in this

55

sense. a measure of the reference stress. such that

$$\sigma_R = \mu \sigma_y. \tag{5.2}$$

The value of μ is less than one prior to collapse and is equal to one when collapse occurs. Through a sequence of plastic hinge formations. the component or structure releases static indeterminacies eventually resulting in a collapse mechanism.

The knowledge of the reference stress is therefore useful in assessing the local as well as remote relaxation behavior of the component. The reference stress can be obtained from the Eq. 5.1 provided the limit load of the component is known. The limit load estimated from inelastic finite element analysis can be used to determine the reference stress. It has been found that the reference stress determined from the r-node method is an upper bound on the exact reference stress. In order to study the relaxation locus in detail. limit load obtained from inelastic finite element analysis is used in conjunction with Eq. 5.1 for evaluating the reference stress.

5.3 Determination of Relaxation Locus

A typical plot of the relaxation locus of a local region for a component subjected to mechanical loading is shown in Fig 5.1. The material is assumed to be elastic-perfectly plastic. From the knowledge of the limit load, the reference stress is obtained, which is specified as the fictitous yield stress in order to carry out the non-linear analysis. Points 1 to 6 in Fig. 5.1 are the stress-strain points corresponding to load increments pertaining to a non-linear finite element analysis. The relaxation locus has to be determined for a constant load, which in this case is the load applied on the structure. P. The stress and strain obtained from the load steps of a non-linear finite element analysis have to be suitably scaled, in order to determine the complete relaxation
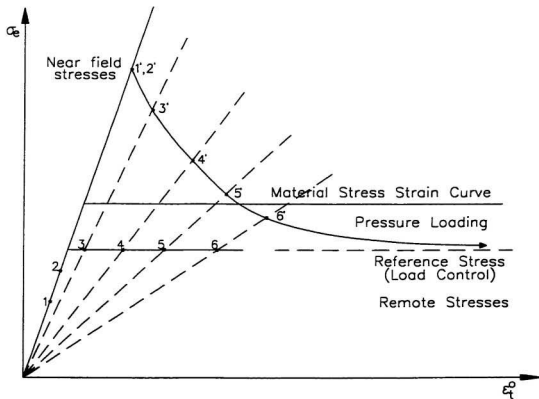
Figure 5.1: Plot of stress relaxation of a mechanical component

locus for the applied load.

Points 1 and 2 corresponding to the first two load steps, lie on the linear elastic line and can be scaled proportionally to the applied load P, to obtain points $1'$ and $2'$. If P_1, σ_{e1} and ϵ_{e1} are the load, stress and strain corresponding to point 1, then the stress-strain point $1'$ can be obtained as

$$\sigma_{e1'} = \frac{P}{P_1}\sigma_{e1} \qquad \epsilon_{e1'} = \frac{P}{P_1}\epsilon_{e1}. \qquad (5.3)$$

Redistribution takes place as soon as the stress in the local region reaches yield. Points 3-6 corresponding to the subsequent load increments can be identified on the stress-strain curve. They can also be suitably scaled in proportion to the load corresponding to the particular loadstep to obtain $3'$-$6'$, even though they lie on the non-linear portion of the stress-strain curve. The scaling is performed by assuming that any inelastic distribution can be obtained by an elastic analysis provided the modulus of elasticity and Poisson's ratio of all the elements are known. The equivalence is described in the following section.

5.4 Elastic-Inelastic Equivalence

Stress-strain relation for an elastic-perfectly plastic material under uniaxial loading is given by

$$\begin{aligned}
\epsilon &= \frac{\sigma}{E} & \sigma < \sigma_y \\
\epsilon &= \frac{\sigma_y}{E} + \epsilon^p & \sigma > \sigma_y
\end{aligned} \qquad (5.4)$$

where σ_y is the yield stress. For a component subjected to combined mechanical and thermal loadings, the total strain tensor is given by

$$\begin{aligned}
\epsilon_{ij} &= \epsilon_{ij}^e + \epsilon_{ij}^p + \epsilon_{ij}^{th} \\
&= \frac{1}{E}\left[(1+\nu)\,\sigma_{ij} - \nu\sigma_{kk}\delta_{ij}\right] + \frac{1}{E_p}\left[\frac{3}{2}\sigma_{ij} - \frac{1}{2}\sigma_{kk}\delta_{ij}\right] + \alpha\Delta T\delta_{ij} \qquad (5.5)
\end{aligned}$$

58

where E_p is the plastic modulus and is given by $\frac{\sigma_y}{\epsilon_p}$. The total strain tensor can be rewritten as

$$\epsilon_{ij} = \left(\frac{1+\nu}{E} + \frac{3}{2}\frac{\epsilon_p}{\sigma_y}\right)\sigma_{ij} - \left(\frac{\nu}{E} + \frac{1}{2}\frac{\epsilon_p}{\sigma_y}\right)\sigma_{kk}\delta_{ij} - \alpha\Delta T\delta_{ij}. \qquad (5.6)$$

If E_s and ν_s are the elastic material properties capable of describing the inelastic behavior. the total or the elastic strain tensor is given by

$$\epsilon_{ij} = \left(\frac{1+\nu_s}{E_s}\right)\sigma_{ij} - \frac{\nu_s}{E_s}\sigma_{kk}\delta_{ij} + \alpha\Delta T\delta_{ij}. \qquad (5.7)$$

Comparing Eqs. 5.6 and 5.7, E_s and ν_s can be obtained as

$$\begin{aligned}
E_s &= \frac{E\sigma_y}{\sigma_y + E\epsilon_p} \\
\nu_s &= \frac{\nu\sigma_y + 0.5E\epsilon_p}{\sigma_y + E\epsilon_p}.
\end{aligned} \qquad (5.8)$$

The above equations provide the complete spatial distribution of material properties to simulate the inelastic behavior from an elastic analysis.

To demonstrate the above equivalence. a thick cylinder under plane strain condition subjected to pressure as well as linear temperature distribution is considered.

- Dimensions of the cylinder :

  Inner Radius, $R_i = 3$ in.

  Outer Radius, $R_o = 9$ in.

- Material Properties :

  Yield Stress, $\sigma_y = 300$ psi

  Modulus of Elasticity, E = 207 ksi

  Coefficient of Linear Thermal Expansion, $\alpha = 1.0 \times 10^{-5}$ per $^\circ C$

- Loadings :

  Inner Surface Temperature = $200^\circ C$

Outer Surface Temperature = $0^{\circ}C$

Applied Internal Pressure = 300 psi

- Number of elements = 25

A non-linear finite element analysis is performed and the element centroidal equivalent stress and strain distributions are shown in Figs. 5.2 and 5.3. Using the equivalent plastic strains from the non-linear analysis results, the modulus of elasticity and Poisson's ratio are modified according to Eq. 5.8 and a linear elastic analysis is performed. It can be seen from Figs 5.2 and 5.3 that the equivalent stress and strain distribution obtained from inelastic and modified elastic analysis are equal.

Therefore, any stress-strain distribution obtained from a non-linear analysis can be obtained from a linear elastic analysis by modifying its modulus of elasticity and Poisson's ratio. This makes it possible to scale the stresses and strains obtained from any load step corresponding to an inelastic analysis, to the applied total load.

5.5 Three Bar Model - Relaxation Locus

As the governing equations are available in simple form for the uniaxial case of bar models, a three bar model subjected to mechanical, thermal and combined loadings is studied. The complete relaxation locus is identified for all the cases and some conclusions are drawn.

- Dimensions of the model :

  Length of bar 1 = 1 m

  Length of bar 2 = 2 m

  Length of bar 3 = 3 m

  Area of all the bars = 1 m^2
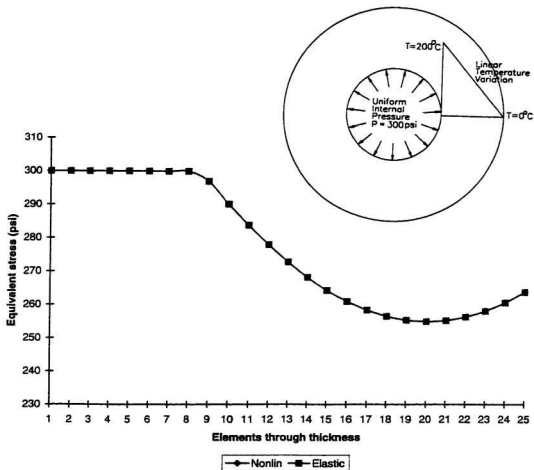
Figure 5.2: Equivalent stress distributions across the radius of a cylinder subjected to uniform internal pressure and a linearly varying temperature
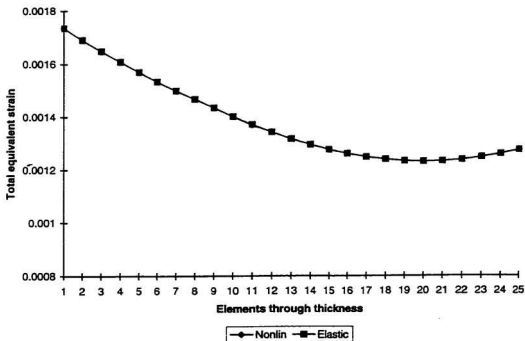
Figure 5.3: Total equivalent strain distributions across the radius of a cylinder subjected to uniform internal pressure and a linearly varying temperature

- Material Properties :

    Yield stress of all the bars = 100 N/m^2

    Modulus of Elasticity = 100 N/m^2

    Coefficient of thermal expansion = 0.02 $per°C$

- Loadings :

    Applied mechanical load. P = 235 N

    Uniform Temperature = 50$°C$

5.5.1 Pressure Loading

The equilibrium equation of a three bar model with equal areas is given by

$$(\sigma_1 + \sigma_2 + \sigma_3) A = P \tag{5.9}$$

where σ_1, σ_2 and σ_3 are the bar axial stresses and P is the applied load. If all the bars are assumed to be elastic-perfectly plastic with same yield stress value. then the limit load of the three bar model can be determined as

$$P_L = 3\sigma_y A. \tag{5.10}$$

Using Eq. 5.1, the reference stress for the applied load. P. is determined as

$$\sigma_R = \frac{P}{3A}. \tag{5.11}$$

A non-linear finite element analysis is performed by specifying the reference stress as the yield stress value. Using the procedure outlined in Sec. 5.3, the relaxation locus is obtained for the given load, P. Fig. 5.4 shows the complete relaxation locus of the local bar (bar 1). As soon as the stress in the local bar reaches yield, any additional applied load is transfered to the remaining bars. The reduction in stiffness of the structure and the redistribution process is identified on the relaxation locus by the

63
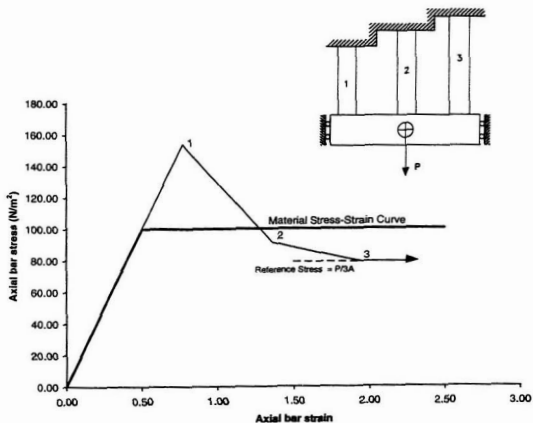
Figure 5.4: Relaxation locus for a three bar model subjected to mechanical loading

line 1-2. At point 2, the stress in bar 2 reaches yield thereby creating further reduction in the stiffness. Line 2-3 shows the stress relaxation of the local bar with increasing strain. When the stress reaches point 3, bar 3 also yields resulting in collapse of the structure.

5.5.2 Temperature Loading

The equilibrium equation of a three bar model subjected to a thermal load is

$$(\sigma_1 + \sigma_2 + \sigma_3)\, A = 0. \tag{5.12}$$

For pure thermal loadings, stresses are set up to equilibriate internally and to satisfy the compatability requirements. The onset of yielding of the local bar initiates the process of redistribution. For a uniform temperature rise in all the bars, it can be seen that a tensile stress is set up in bar 1 and compressive stresses are set up in bars 2 and 3, in order to satisfy the compatability requirements. As the magnitude of the tensile stress in bar 1 is more than bars 2 and 3, bar 1 is considered as the local bar. Consequently, bar 1 yields in tension first followed by bar 3 in compression. At this temperature the structure is in equilibrium, with bar 2 remaining stress free. Further increases in temperature produce equal strains increments $(\alpha \Delta T)$ in all the bars proportional to the temperature rise ΔT with no change in the bar stresses.

Collapse does not occur in structures subjected to pure thermal loadings, as equilibrium is preserved internally by redistribution of stresses. Therefore, any arbitrary value of yield stress can be prescribed in order to determine the complete relaxation locus from a non-linear finite element analysis. For the three bar model a yield stress value of 20 N/m^2 is prescribed. On the relaxation locus diagram, line 1-2 corresponds to the relaxation of stress after the yielding of bar 1. Redistribution takes place until point 2 after which bar 3 yields in compression. Further increases in the temperature will cause the axial stress in bar 1 to relax from 2 to 3 without any change in strain.
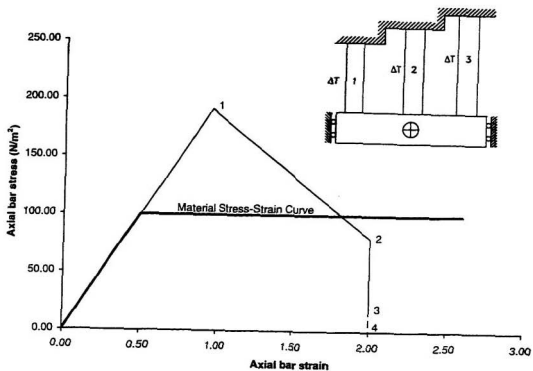
Figure 5.5: Relaxation locus for a three bar model subjected to temperature loading
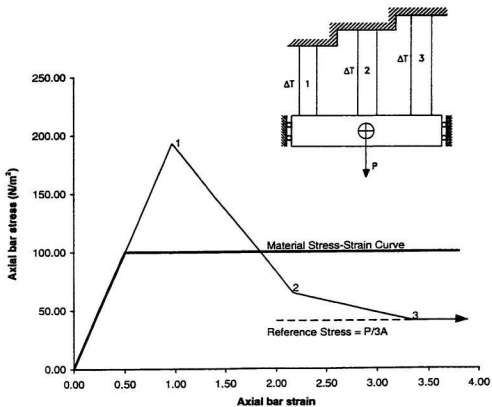
Figure 5.6: Relaxation locus for a three bar model subjected to combined mechanical and thermal loading

It can be seen that the relaxation of stress with non-increasing strain would continue for any arbitrary low value of yield stress (shown by dotted line 3-4).

For combined loadings. (Fig. 5.6) the relaxation locus is very similar to pressure loading case as a reference stress can be identified to balance the external load.

It was shown earlier in Chapter 4, that the inelastic strain predicted by the modulus modification method and the analytical method were equal for the case of two bar model. From the relaxation locus diagrams it can be seen that for all loading cases, the relaxation is linear for a certain drop in stress level. For small load cases, where the first linear portion of the relaxation locus intersects the material stress-strain curve, accurate predictions are made by the modulus modification method.

5.6 General Pressure Component Relaxation Locus - Pressure and Thermal Loadings

Figs. 5.7 and 5.8 are the relaxation locus curves for a plate with central hole and a Bridgman notch respectively. The relaxation locus curves for pressure loading are similar to the case of bar models. As yielding progresses, the stiffness of the structure reduces thereby producing more strain at the local element. For the applied load, P, collapse state corresponds to the yield being set at a value of the reference stress. The relaxation curve for pure thermal loading, in the case of Bridgman notch, shows decreasing strain increments as the stress relaxes. As in the case of bar models, the structure approaches an equilibrium point. In the case of the plate with a hole, convergence could be obtained only with the yield stress value of 100 MPa. The increasing strain at the local region is attributed to the fact that more than half the elements were still elastic.

The relaxation curve for a general pressure component can be identified as multi-bar model with plasticity gradually proceeding from the shorter bar to the longer bar
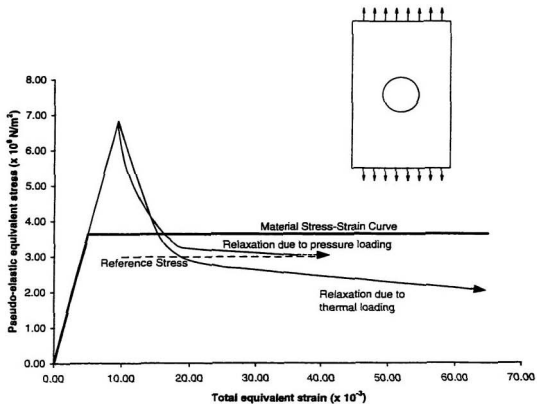
Figure 5.7: Relaxation locus for a plate with a hole subjected to pressure and thermal loads
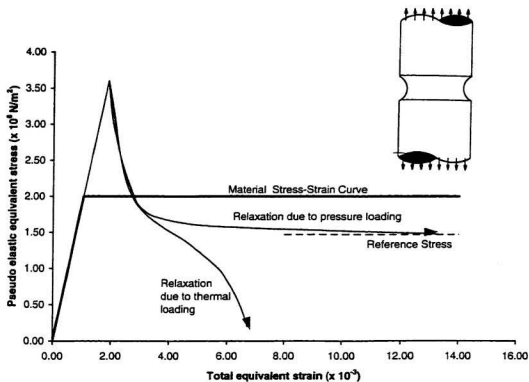
Figure 5.8: Relaxation locus for a Bridgman notch subjected to pressure and thermal Load
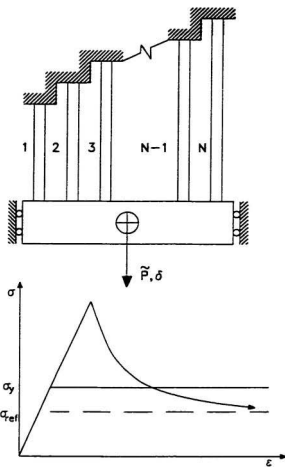
Figure 5.9: Relaxation locus for a multi-bar model subjected to pressure loading

as shown in Fig. 5.9. The relaxation locus of the model can be obtained as a series of lines with decreasing slopes eventually converging at the reference stress.

5.7 Neuber's Relaxation Locus

Neuber's rule states that the theoretical stress-concentration factor is the geometric mean of the actual stress and strain concentration factors. Although this *approximation strictly holds for specific notch constraints*, on account of its simple form and ease of use, it has been extended to predict notch root strains for other geometric configurations in its equivalent form.

Neuber's relaxation locus is described by the equation

$$\sigma_e \epsilon_{eqv} = \text{constant}. \tag{5.13}$$

If σ_{e1} and ϵ_{e1} are the notch root pseudoelastic equivalent stresses and strains and if ϵ_N is the inelastic strain predicted by Neuber's rule, then, for an elastic-perfectly plastic material we have

$$\sigma_{e1} \epsilon_{e1} = \sigma_y \epsilon_N. \tag{5.14}$$

Therefore, the implied GLOSS angle θ is given by:

$$\begin{aligned}
\tan \theta &= \left(\frac{\epsilon_N}{\epsilon_{e1}} - 1 \right) \bigg/ \left(1 - \frac{\sigma_{e1}}{\sigma_y} \right) \\
&= \frac{\sigma_{e1}}{\sigma_y}. \tag{5.15}
\end{aligned}$$

The relaxation-modulus $\overline{E}_r = -\tan\left(\frac{\pi}{2} - \theta\right)$. The GLOSS angle θ for Neuber's case is a function of the maximum elastic stress and yield stress and for given loading conditions, it is, independent of the geometry.

It has been shown by experiments that Neuber's rule predict strains higher than the measured strains for many cases other than thin sheets. Similar observations have been made by Mowbray and Ohji [22, 26]. It has also been shown that Neuber's

72
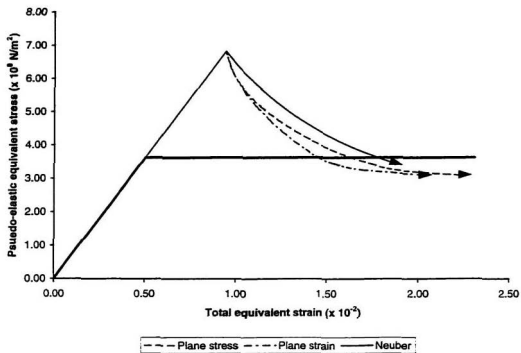
Figure 5.10: Relaxation locus for a thin plate with a hole subjected to plane stress and plane strain conditions

rule agrees well with measurements in plane stress situations such as thin sheets in tension.

Fig. 5.10 is the relaxation plot of a plate with a central hole subjected to pressure loading. The figure shows the relaxation of the local element when the plate is under plane stress condition and plane strain condition. It can be seen that for the same maximum stress and yield stress, the relaxation of the two curves are different on account of the constraint prevailing at the vicinity of the notch. The strain estimated by the plane strain case is less than the plane stress condition. For both cases, Neuber's rule predicts the same strain. Neuber's rule takes into account only the maximum stress and the yield, and the local inelastic strain does not depend on the constraint. This is obviously a drawback of Neuber's rule.

5.8 GLOSS for combined loadings

The relaxation locus is identical for both mechanical and thermal loadings for a limited drop in stress level. It is seen that thermal loadings also behave as mechanical load, with redistribution of stress occurring after the yield initiation. It is also found that the actual plastic zone is larger than the nominal plastic zone. Therefore, the GLOSS with Plasticity Correction modulus modification scheme presented in Chapter 3, can also be used for thermal as well as combined mechanical and thermal loadings.

As well, it was shown earlier in Eq. 5.8 that modulus as well as Poisson's ratio are modified in order to simulate the non-linear finite element analysis from an elastic analysis. In order to obtain improved estimate of strains predicted by the GLOSS method with Plasticity Correction, the Poisson's ratio of each elements above nominal yield is also modified to 0.49. This essentially assumes all the elements above yield from the first analysis to be completely plastic leading to better inelastic strain

74

estimates.

Chapter 6

Numerical Examples

6.1 Introduction

The GLOSS method with Plasticity Correction (GMPC) is applied to some benchmark geometric configurations and an industrial problem of practical interest. The configurations analyzed have notch-type details wherein the determination of inelastic strain is useful in estimating the low-cycle fatigue life. Inelastic strain at the notch root is obtained by the GMPC, which is used in conjunction with the cyclic stress-strain curve of the material. The estimated strain can then be inserted into the Coffin-Manson's strain life equation in order to determine the number of cycles required for crack initiation.

The numerical examples considered are :

- a plate with a hole

- a Bridgman notch

- an axisymmetric cylinder with a circumferential notch on the inside surface and

- a steam turbine valve body.

These components are modeled using ANSYS finite element software and are subjected to mechanical, thermal and combination loadings. The materials used are

assumed to be homogeneous, isotropic and elastic-perfectly plastic. The inelastic strain estimated by the GMPC is compared with inelastic finite element results and Neuber's rule.

6.2 Thin Plate with a Hole

A thin plate with a circular hole is subjected to a remote tensile stress. On account of symmetry only one quarter of the plate is modeled using four noded isoparametric quadrilateral elements. Next the plate is fixed on the top surface and is subjected to a uniform and linearly varying temperature.

- Dimensions of the Plate :

    Length of the plate $= 0.7620 \times 10^{-1}$ m

    Width of the plate $= 0.3819 \times 10^{-1}$ m

    Radius of the hole $= 0.6375 \times 10^{-2}$ m

- Material Properties :

    Material - 24S-T3 Aluminum Alloy

    Modulus of Elasticity, $E = 7.2368 \times 10^{4}$ MPa

    Yield Stress, $\sigma_y = 363.2$ MPa

    Coefficient of Linear Thermal Expansion $= 3 \times 10^{-5}$ per $^{\circ}C$

Figures 6.1, 6.2 and 6.3 are the plots of notch root pseudoelastic equivalent stress (the theoretical notch stress, $\sigma_n K_t$) versus the notch root total equivalent strain. For various pressures and temperatures, the inelastic strain estimates are determined by the GMPC and non-linear finite element analysis. Since uniaxial state of stress exists at the notch root, Neuber's rule gives good predictions of the inelastic strain. It can be seen from the plots that the strains estimated by the GMPC agree reasonably well with the non-linear finite element results. Although the strain is underpredicted for

certain load cases, the maximum error is found to be not more than three percent, which would result in not very unconservative fatigue life. Further, the time involved in performing a non-linear analysis was found to be 4-6 times more than that required by GMPC. From the plots, it can also be seen that the GMPC shows similar behavior for pressure as well as thermal loading cases.

6.3 Bridgman Notch

A round bar with a deep circumferential notch under tensile load is considered as an example of biaxially stressed notches. The radial stress at the notch root is zero due to the free surface, and in addition, the circumferential strain is also zero since the notch radius ρ is small compared to the other dimensions. The problem considered here is that of a plane strain condition. Advantage is taken of the symmetry present and therefore only one quarter of the notch is modeled.

- Dimension of the Bridgman Notch :
  Maximum diameter $= 2.6416 \times 10^{-2}$ m
  Minimum diameter $= 2.1082 \times 10^{-2}$ m
  Notch radius $= 0.6858 \times 10^{-2}$ m

- Material Properties :
  Material = Cr-Mo Steel
  Yield stress, $\sigma_y = 200.00$ MPa
  Modulus of Elasticity, $E = 1.9 \times 10^5$ MPa
  Coefficient of Linear Thermal Expansion, $\alpha = 1.5 \times 10^{-5}$ per ^oC

Figures 6.4 and 6.5 are the plots of pseudo elastic equivalent stress, (the theoretical notch root equivalent stress, $\sigma_n K_t$) versus the notch root total equivalent strain. As it can be seen from the graph, for a given value of load or temperature the inelastic
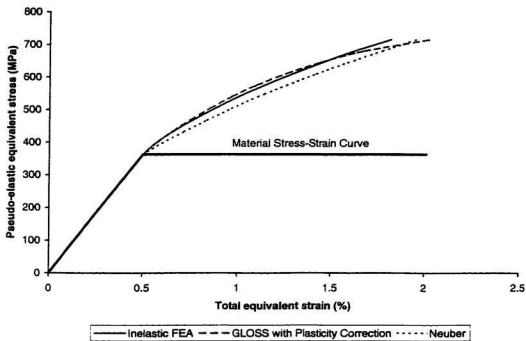
Figure 6.1: Plate with a Hole - Plastic Strain concentration due to Pressure Load
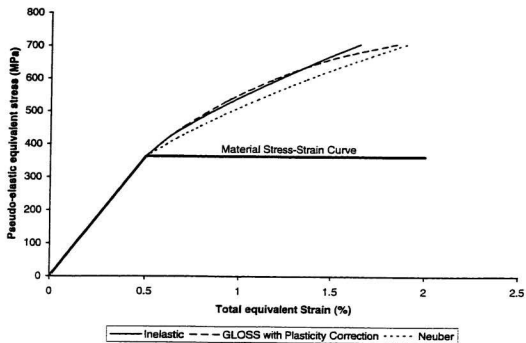
Figure 6.2: Plate with a Hole - Plastic Strain concentration due to Uniform Temperature
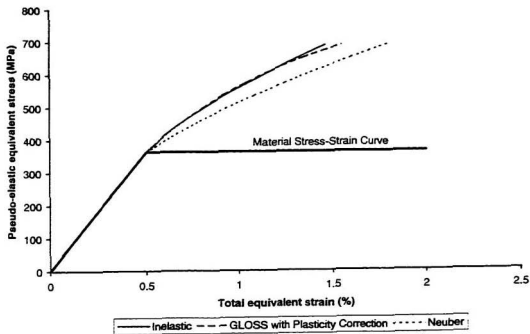
Figure 6.3: Plate with a Hole - Plastic Strain concentration due to Linearly Varying Temperature

strain predicted by the GMPC overestimates the strain predicted by the inelastic finite element results leading to conservative low-cycle fatigue life. It can also be seen that Neuber's rule overestimates the strain by around 25% leading to overly conservative fatigue life.

6.4   Cylinder with a Circumferential Notch

In order to demonstrate the application of the proposed method to triaxially stressed notches, a thick-walled cylinder with a circumferential notch on the inside surface under internal pressure is considered. The cylinder is subjected to a plane strain condition. The cylinder is subjected to pressure loading and combined pressure and uniformly varying thermal loading.

- *Dimensions of the Cylinder :*

  Outer diameter = 50 in.

  Inner diameter = 32 in.

  Notch radius = 1 in.

- Material Properties :

  Yield stress, $\sigma_y = 29000$ psi

  Modulus of Elasticity, $E = 27.5 \times 10^6$ psi

  Coefficient of linear thermal expansion = 3×10^{-5} per °C

Figures 6.6 and 6.7 shows the notch root equivalent strain results for various pressure and combined loads. Once again. it can be seen that the strain estimated by the GMPC somewhat overpredicts the non-linear results but is not as conservative as Neuber's rule.

From the above three examples it can be seen that the GLOSS method with Plasticity Correction predicts reasonably accurate inelastic strain, and is conservative from a fatigue standpoint for most of the cases.
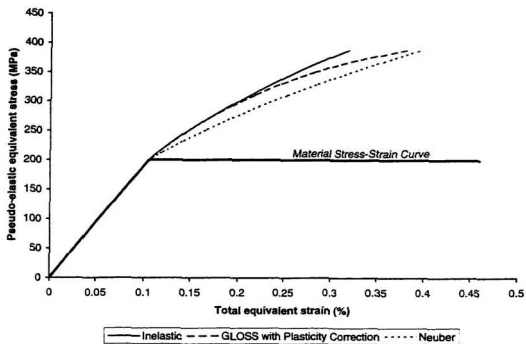
Figure 6.4: Bridgman Notch - Plastic strain concentration due to Mechanical Load
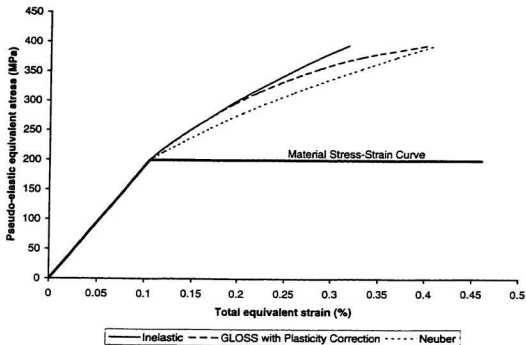
Figure 6.5: Bridgman Notch - Plastic strain concentration due to Uniform Temperature
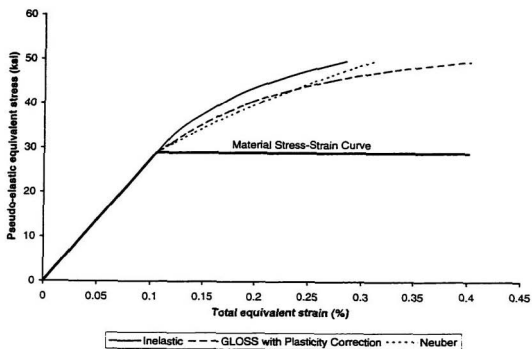
Figure 6.6: Cylinder with a Circumferential Notch - Plastic strain concentration due to Pressure Load
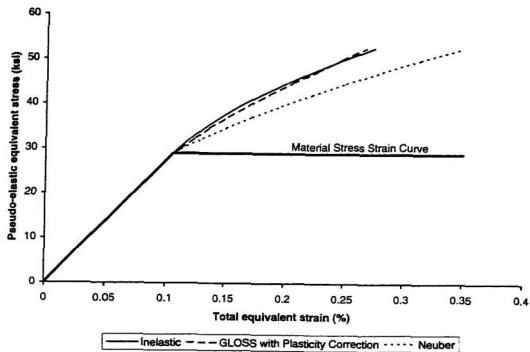
Figure 6.7: Cylinder with a Circumferential Notch - Plastic strain concentration due to combined Pressure and Thermal Load

6.5   Steam Turbine Valve Body

Having demonstrated the validity of the robust method for benchmark problems, a problem of practical interest to designers of power plants is analyzed next.

The need for increased thermal efficiency and improved use of resources has led to higher operating temperatures and pressures. The concurrent presence of cyclic secondary stresses (discontinuity and thermal stresses) and sustained primary stresses (pressure-induced and mechanical loads) could cause plastic strains to be incurred during every cycle of start-up and shut-down, along with temperature transients. The components are thus subjected to cyclic nature of stresses which consequently result in low-cycle fatigue failure of the components.

In order to reduce the damage caused by fatigue and to ensure safe operation of turbine components for a specific period, it is essential that the thermal strains in components during start-up and shut-down periods be not allowed to exceed limiting values obtained from their respective material fatigue curves. In other words, start-up and load change rates are to be governed by the permissible magnitude of thermal strains in the turbine and valve components.

The most important factors for determining the start-up rates are

- identification of the critical section

- evaluation of peak strains at the critical section

A section which comes into contact with high temperature steam, or sections with sharp geometry can be expected to be a critical section. The peak stresses can be determined by an elastic finite element analysis. The highest stressed element from the elastic finite element analysis is considered as the critical location.

Evaluation of temperature at various times during transient operation is the first step of thermal stress analysis. ANSYS finite element software is used to solve for

Ø390
Ø540
15
Ø200
210
Ø165
R63 R50
R10
Ø360
Ø225
40
25
150
Ø200
300
460
Ø230
250
Ø390
Ø580
1055
725
625.5
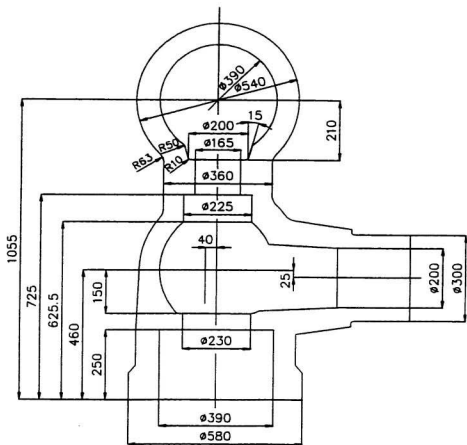
(All Dimensions are in mm)

Figure 6.8: Steam turbine valve body - Dimensions

88

Critical
Section
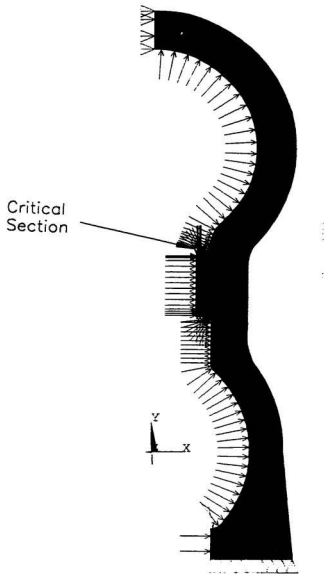
Figure 6.9: Steam turbine valve body - Finite element model

the temperature at various times, and stresses corresponding to the temperature distributions, in this problem of heat conduction and stress analysis. The initial temperature of all points in valve body before starting up from cold is taken as 30°. The valve is ramped to a steam temperature of 500°C for different start up times. Inelastic strains are estimated for the different start-ups to determine the longest life.

The dimensions of the valve body are shown in Fig. 6.8 and the finite element model is shown in Fig. 6.9.

- Material Properties :

  Material - Cr-Mo Steel

  Yield Stress = 300 MPa

  Modulus of Elasticity = 1.8521×10^5 MPa

  Coefficient of linear thermal expansion, $\alpha = 1.5022 \times 10^{-5}$ per °C

  Inner surface convective heat transfer coefficient = $3000 J/sec - m^2 - ° K$

The valve body is modeled using 6 noded triangular axisymmetric elements. The temperature at the inner surface is gradually increased to the steam temperature of 500 °C. Valve bodies are normally lagged with thermal insulation so that the heat loss can be minimized. The outer surface is modeled such that the heat flux is zero.

A transient heat conduction analysis is first carried out to determine the temperature distribution at various times during the start-up. The maximum thermal stress occurring in the valve body depends on the duration of the start-up. The temperature difference at the critical section where the maximum stress occurs for various start-up durations is shown in Table 6.1.

Using the temperature distributions at various times during the start-up, a structural analysis is performed to determine the inelastic strain. The strains are estimated by non-linear finite element analysis, GLOSS method with Plasticity Correction and Neuber's rule. The strain estimates are shown in Table 6.2. It can be seen that the

90

Table 6.1: Temperature difference at the critical section

Start-up Time (secs)	1500	2000	2500
Temperature Difference $^{\circ}C$	186	160	145

strain estimated by the GLOSS method with Plasticity Correction in conjunction with the Poisson's ratio modification are comparable with the detailed inelastic analysis and are conservative from a fatigue standpoint. It can also be seen that Neuber's rule underpredicts the inelastic strain for all cases. This aspect of non-conservativeness of Neuber's rule is not widely known.

Table 6.2: Steam Turbine Valve Body - Inelastic Strain Estimates

Pressure (MPa)	Temperature Difference ($^{\circ}C$)	Elastically Calculated Strain (Percent)	Inelastic Strain (Percent)			
			Neuber	GLOSS		Inelastic FEA
				$\nu = 0.3$	$\nu = 0.49$	
5.0	186	0.308	0.587	0.714	1.170	0.692
9.81	186	0.297	0.546	0.596	0.991	0.649
13.73	186	0.288	0.513	0.536	0.860	0.619
5.0	160	0.260	0.418	0.428	0.618	0.512
9.81	160	0.249	0.383	0.387	0.568	0.467
13.73	160	0.240	0.356	0.358	0.517	0.433
5.0	145	0.231	0.328	0.331	0.457	0.401
9.81	145	0.220	0.298	0.298	0.418	0.360
13.73	145	0.210	0.274	0.274	0.382	0.339

Chapter 7

Conclusions and Future Research

7.1 Conclusions

The determination of inelastic strain at a critical section of any mechanical component or structure is required for evaluating the fatigue life of components. Most of the components in power plants and process industries are often subjected to combined mechanical and thermal loadings. In such highly competitive environments, simple and reliable methods are necessary during the preliminary stages of design.

Conventional methods such as non-linear finite element analysis are expensive and time consuming and are not suitable for such practical situations. Caution should be exercised when using simple methods such as Neuber's rule. Neuber's rule predicts reasonably accurate strains only for the plane stress case such as thin sheets. In plane strain situations Neuber's rule has been found to overestimate the actual inelastic strain significantly leading to overly conservative fatigue lives. Also, it is shown in this thesis that for the case of steam turbine valve body, the strain predicted by Neuber's rule underestimates the non-linear results.

Fully cognizant of the difficulties inherent in conventional methods, this thesis aimed to develop a simple method for evaluating the inelastic strain in any component subjected to combined mechanical and thermal loadings. Fundamental aspects of the modulus reduction method are explained through a two-bar kinematic model. A pro-

cedure has been developed to obtain the complete relaxation locus of any component subjected to mechanical and thermal loadings. It is shown that any inelastic analysis can be exactly simulated by an elastic analysis provided the modulus of elasticity and Poisson's ratio distributions are known. In addition to identifying the redistribution process. the relaxation locus also predicts the local inelastic strain and the reference stress. The relaxation locus is identified for the bar models and some general mechanical components. It is found that the relaxation locus for pure thermal loading is identical to that of pressure loading for a limited drop in stress level. Based on the similar nature of the relaxation locus. the GLOSS method with Plasticity Correction has been extended to combined mechanical and thermal loadings.

The method has been applied to some bench-mark problems and practical steam turbine valve body problem. The inelastic strain estimated by the GLOSS method with Plasticity Correction compares favorably with non-linear finite element results. The method developed can be applied to any component configuration as the relaxation depends on the geometry and multiaxiality conditions existing at the critical section, which is not taken into account in Neuber's rule.

7.2   Future Research

It is shown in this thesis that the robust method is simple and direct, and provides good estimates of inelastic strain for combined loading cases. Further research in this area should be worthwhile. Determination of bounds should be an area worth pursuing as it would be a measure of conservativeness of the design. Future research should concentrate on extending the method towards orthotropic and anisotropic components, which play an important role in engineering due to their superior strength to weight characteristics.

References

[1] Adinarayana. N., and Seshadri. R., "Simplified Thermal Fatigue Evaluations using the GLOSS method." *ASME-PVP Conference*, PVP Volume. 323. Montreal. Canada, 1996.

[2] *ANSYS Engineering Analysis System User's Manual*, Rev. 5. Swanson Analysis Systems Inc.. Houston, Pa.. 1992.

[3] *ASME Boiler and Pressure Vessel Code*, American Society of Mechanical Engineers, 1989.

[4] *Annual Book of ASTM Standards*. American Society for Testing and Materials, 1990.

[5] Calladine. C. R., *Engineering Plasticity*, Pergamon Press, Oxford, 1969.

[6] Collins, J. A., *Failure of Materials in Mechanical Design*, John Wiley & Sons, 1993.

[7] Dhalla, A. K., "A Simplified Procedure to Classify Stresses for .Elevated Temperature Service," *Proceedings of the ASME-PVP*, San Diego, Vol. 120, pp. 177-188, 1987.

[8] Dhalla, A. K., and Jones, G. L., "ASME Code Classification of Pipe Stresses: A Simplified Elastic Procedure," *International Journal of Pressure Vessel and Piping*, Vol. 26, pp. 145-166, 1986.

[9] Dowling, N. E.. "A Discussion of Design Methods for Estimating Fatigue Life," *Proceedings of the SAE Fatigue Conference, Society of Automotive Engineers,* Warrandale. PA. pp. 109. 1982.

[10] Dowling, N. E.. *Strength of Materials - Deformation Fracture and Fatigue.* McGraw-Hill. 1994.

[11] Gill. S. S.. *The Stress Analysis of Pressure Vessels and Pressure Vessel Components.* Pergamon Press. 1970.

[12] Hill. R.. *The Mathematical Theory of Plasticity,* Oxford University Press. New York. 1971.

[13] Hoffman and Seeger. P.. "Multiaxial Elaso-Plastic Stress Strain Relationships," *Journal of Testing and Evaluation,* Vol. 10. No.4. pp. 199-204. 1985.

[14] Johnson. W., and Mellor. P. B.. *Engineering Plasticity,* Ellis Horwood Limited. 1983.

[15] Kizhatil. R. K.. and Seshadri. R.. "Inelastic Strain Concentration factors and Low Cycle Fatigue of Pressure Components using GLOSS Analysis." *ASME PVP.* San Diego. Vol. 210-2. pp. 149-154. 1991.

[16] Kizhatil. R. K.. and Seshadri. R.. "Multiaxial stress relaxation using the local region constraint parameter," *International Journal of Pressure Vessels and Piping,* Vol. 63, pp. 99-110, 1995.

[17] Kraus. H.. *Creep Analysis,* John Wiley & Sons, 1980.

[18] Manson. S. S., *Thermal Stress and Low Cycle Fatigue,* McGraw-Hill, New York, 1966.

[19] Mendelson, A., *Plasticity: Theory and Application*. The Macmillan Company, New York. 1968.

[20] Molski, K., and Glinka, G., "A Method of Elastic-Plastic Stress and Strain Calculation at a Notch Root," *Material Science Engineering*, Vol. 50. pp. 93-100. 1981.

[21] Moftakar and Glinka, G., "Multiaxial Elasto-Plastic Notch Strain Analysis," *Journal of Fracture Mechanics*. 1993.

[22] Mowbray, D. F., and Mc Connelee, J. E., "Application of finite element elastic-plastic analysis to notched fatigue specimens," *First International Conference on Reactor Structural Mechanics*. Berlin. 1970.

[23] Neuber, H., "Theory of Stress Concentration for Shear-Strained Prismatical Bodies with Aribitrary Nonlinear Stress-Strain Laws," *Transactions of the ASME: Journal of Applied Mechanics*. Vol. E28. pp. 544. 1965.

[24] R5. *Assessment Procedure for High Temperature Response of Structures*. Nuclear Electric, Berkeley Nuclear Laboratories. 1990.

[25] R6. *Assessment of the Integrity of Structures containing Defects*. Nuclear Electric, Berkeley Nuclear Laboratories. 1990.

[26] Ohji, K., Ogura, K., and Takii, H., "Elastic-plastic analysis of notched specimens using the finite element method," *14th Congress of Japan materials research*. Kyoto, Japan, 1971.

[27] Kizhatil, R., *Robust Approximate Methods for Inelastic Analysis of Mechanical Components*, Ph. D Thesis, University of Regina, Regina, Canada.

[28] Seeger. T.. and Heuler, P.. "Generalized Application of Neuber's Rule." *Journal of Testing and Evaluation*. Vol. 8. No. 4. pp. 199-204. 1980.

[29] Seshadri, R.. "The Generalized Local Stress Strain (GLOSS) Analysis - Theory and Applications." *25th Anniversary Volume, ASME Journal of Pressure Vessel Technology*, pp. 219-227. 1991.

[30] Seshadri, R.. "Classification of Stress in Pressure Components using the 'GLOSS' Diagram." *Proceedings of the ASME PVP, Nashville.* Vol. 186. pp. 115-123. 1990.

[31] Seshadri. R.. "The Effect of Multiaxiality and Follow-up on Creep Damage." *Journal of Pressure Vessel Technology*, Vol. 112. pp. 378-385. 1990.

[32] Seshadri. R.. "Simplified Methods for determining Multiaxial Relaxation and Creep Damage," *ASME PVP*. San Diego, Vol. 210-2. pp. 173-180. 1991.

[33] Seshadri. R., and Kizhatil. R. K.. "Inelastic Analyses of Pressure Components using the 'GLOSS' Diagram." *Proceedings of the ASME PVP. Nashville.* Vol. 186. pp. 105-113, 1990.

[34] Seshadri. R.. and Kizhatil. R. K.. "Notch Root Inelastic Strain Estimates Using GLOSS Analysis," *Advances in Multiaxial Fatigue*. ASTM STP 1191. D. L. McDowell and R. Ellis, Eds.. American Society for Testing and Materials. Philadelphia, pp. 397-411, 1993.

[35] Seshadri. R., and Marriott, Dl. L., "On Relating the Reference Stress. Limit Load and the ASME Stress Classification Concepts," *International Journal of Pressure Vessels and Piping*, Vol. 56, pp. 387-408, 1993.

[36] Seshadri. R.. and Mikulcik. E. C.. "On Relating Multiaxial and Uniaxial Stress Relaxation in Pressure Components." *Transaction of the CSME.* Vol. 13. No. 1/2. 1989.

[37] Severud. L. K.. "A Simplified Method Evaluation for Piping Elastic Follow-up," *Proceedings of the 5th International Congress of Pressure Vessel Technology.* ASME, San Fransisco. pp. 367-387. 1984.

[38] Sim. R. G.. "Reference Stress Concepts in the Analysis of Structures During Creep." *International Journal of Mechanics and Sciences.* Vol. 12. pp. 561-573. 1970.

[39] Topper. T. H.. Wetzel. R. M.. and Morrow, J. D.. "Neuber's Rule Applied to Fatigue of Notched Specimens." *Journal of Materials.* Vol. 4. No. 1, 1969.

Appendix A

ANSYS Commands Listing of Mechanical Components and Structures

All ANSYS commands listing for the problems given in Chapter 6 are provided in this section. The listings include linear elastic analysis and non-linear analysis using ANSYS. The transient heat conduction analysis performed for the valve body problem is also provided.

A.1 Plate with a Hole - Mechanical Load

A.1.1 Linear Elastic Analysis

```
/BATCH


*SET,STRS,-200e06      ! LOAD ON THE STRUCTURE

*SET,R,6.375e-03       ! RADIUS OF THE CENTRAL HOLE

*SET,W,19.05e-03       ! WIDTH OF THE PLATE

*SET,D,38.1e-03        ! LENGTH OF THE PLATE
```

```
*SET,YS,363.2e06      ! YIELD STRENGTH (psi)

*SET,YM,7.2368e10     ! YOUNG'S MODULUS (psi)

*SET,POISSON,0.3      ! POISSON'S RATIO


/PREP7                ! ENTER PREPROCESSOR

/TITLE, PLATE WITH A CENTRAL HOLE


ET,1,42               ! ELEMENT TYPE - PLANE 42 FOUR NODED

                      ! ISOPARMETRIC QUADRILATERAL ELEMENT

MP,EX,1,YM            ! YOUNG'S MODULUS

MP,NUXY,1,POISSON     ! POISSON'S RATIO


K,1,R,0               ! DEFINITE KEYPOINTS AND LINES

K,2,W,0

L,1,2,22,22

K,3,W,D/2

L,2,3,12

K,4,0,D/2

L,4,3,12

K,5,0,R

L,5,4,22,22

CSYS,1

K,6,R,45

L,5,6,12

L,6,1,12

CSYS,0
```

```
L,6,3,22,22

CSYS,0
K,7,W,D
K,8,0,D
L,3,7,10
L,4,8,10
L,7,8,12

A,1,2,3,6              ! DEFINE AREAS
A,6,3,4,5
A,3,7,8,4
AMESH,ALL             ! MESH THE AREAS WITH ELEMENTS

CSYS,0               ! BOUNDARY CONDITIONS
NSEL,S,LOC,Y,0
D,ALL,UY,0
NALL

NSEL,S,LOC,X,0
D,ALL,UX,0
NALL

SAVE                 ! SAVE MODEL AND GEOMETRY
FINI                 ! EXIT PRE-PROCESSOR
```

```
/SOLU                 ! ENTER SOLUTION
ANTYPE,0              ! STATIC ANALYSIS

NSEL,S,LOC,Y,D        ! APPLY EXTERNAL LOAD
SF,ALL,PRES,STRS
NALL

SAVE                  ! SAVE
SOLVE                 ! SOLVE
FINI                  ! EXIT SOLUTION

/INP,GLOSSMAC         ! INPUT MACRO FOR PERFORMING GLOSS ANALYSIS
EXIT
```

A.1.2   Non-Linear Analysis

```
/BATCH

*SET,STRS,-200E06
*SET,R,6.375E-03
*SET,W,19.05E-03
*SET,D,38.1E-03

*SET,NWID,22
*SET,SRATIO,22
```

```
*SET,YS,363.2E06

*SET,YM,7.2368E10

*SET,POISSON,0.3


/PREP7


ET,1,42

MP,EX,1,YM

MP,NUXY,1,POISSON


TB,BKIN,1,1              ! BI-LINEAR KINEMATIC HARDENING

TBDATA,1,YS,0           ! YIELD STRESS = YS & TANGENT MODULUS = 0


K,1,R,0

K,2,W,0

L,1,2,22,22

K,3,W,D/2

L,2,3,12

K,4,0,D/2

L,4,3,12

K,5,0,R

L,5,4,22,22

CSYS,1

K,6,R,45

L,5,6,12

L,6,1,12
```

```
CSYS,0
L,6,3,22,22


CSYS,0
K,7,W,D
K,8,0,D
L,3,7,10
L,4,8,10
L,7,8,12


A,1,2,3,6
A,6,3,4,5
A,3,7,8,4
AMESH,ALL


CSYS,0
NSEL,S,LOC,Y,0
D,ALL,UY,0
NALL


NSEL,S,LOC,X,0
D,ALL,UX,0
NALL
SAVE


/SOLU
```

```
ANTYPE,0

AUTOTS,ON              ! NON-LINEAR ANALYSIS OPTIONS
PRED,ON,,ON
NROPT,1,,OFF
OUTRES,ALL,ALL

NSUBST,300
TIME,4

NSEL,S,LOC,Y,D
SF,ALL,PRES,STRS
NALL

SAVE
SOLVE

FINISH

/POST1                 ! ENTER POST-PROCESSOR
SET,LAST               ! GO TO THE LAST-SUBSTEP
ETABLE,SEQV,S,EQV      ! STORE THE ELEMENT CENTROID
                       ! EQUIVALENT STRESS
ETABLE,EL,EPEL,EQV     ! STORE THE ELEMENT CENTROID
                       ! ELASTIC EQUIVALENT STRAIN
ETABLE,EP,EPPL,EQV     ! STORE THE ELEMENT CENTROID PLASTIC
```

```
                            ! EQUIVALENT STRAIN
/OUT,RESULTS                ! CREATE OUTPUT FILE
PRETAB,SEQV,EL,EP           ! RE-DIRECT ALL THE RESULTS TO THE FILE
/OUT


FINI
EXIT,NOSAVE
```

A.2 Plate with a Central Hole - Uniform Temperature

A.2.1 Linear Elastic Analysis

```
/BATCH


*SET,R,6.375E-03
*SET,W,19.05E-03
*SET,D,38.1E-03


*SET,YS,363.2E06
*SET,YM,7.2368E10
*SET,ALPHA,3E-05
*SET,TEMP,110


/PREP7
```

```
ET,1,42
MP,EX,1,YM
MP,ALPX,1,3E-05     ! CO-EFFICIENT OF THERMAL EXPANSION


K,1,R,0
K,2,W,0
L,1,2,22,22
K,3,W,D/2
L,2,3,12
K,4,0,D/2
L,4,3,12
K,5,0,R
L,5,4,22,22
CSYS,1
K,6,R,45
L,5,6,12
L,6,1,12
CSYS,0
L,6,3,22,22


CSYS,0
K,7,W,D
K,8,0,D
L,3,7,10
L,4,8,10
L,7,8,12
```

```
A,1,2,3,6
A,6,3,4,5
A,3,7,8,4
AMESH,ALL

CSYS,0
NSEL,S,LOC,Y,0
D,ALL,UY,0
NALL

NSEL,S,LOC,X,0
D,ALL,UX,0
NALL

NSEL,S,LOC,Y,D
D,ALL,UY,0
NALL

SAVE

/SOLU
ANTYPE,0

BF,ALL,TEMP,TEMP      ! TEMPERATURE ARE INPUT AS BODY FORCES
                     ! ON ALL NODES
```

```
SAVE

SOLVE


FINISH

/INP,GLOSSMAC
```

A.2.2   Non-Linear Analysis

```
/BATCH


*SET,R,6.375E-03

*SET,W,19.05E-03

*SET,D,38.1E-03


*SET,YS,363.2E06

*SET,YM,7.2368E10

*SET,TEMP,110


/PREP7


ET,1,42

MP,EX,1,YM

MP,ALPX,1,3E-05


TB,BKIN,1,1

TBDATA,1,YS,0
```

```
K,1,R,0
K,2,W,0
L,1,2,22,22
K,3,W,D/2
L,2,3,12
K,4,0,D/2
L,4,3,12
K,5,0,R
L,5,4,22,22
CSYS,1
K,6,R,45
L,5,6,12
L,6,1,12
CSYS,0
L,6,3,22,22

CSYS,0
K,7,W,D
K,8,0,D
L,3,7,10
L,4,8,10
L,7,8,12

A,1,2,3,6
A,6,3,4,5
```

```
A,3,7,8,4
AMESH,ALL


CSYS,0
NSEL,S,LOC,Y,0
D,ALL,UY,0
NALL


NSEL,S,LOC,X,0
D,ALL,UX,0
NALL


NSEL,S,LOC,Y,D
D,ALL,UY,0
NALL


SAVE


/SOLU
ANTYPE,0


AUTOTS,ON
PRED,ON,,ON
NROPT,1,,OFF
OUTRES,ALL,ALL
```

```
TIME,4
NSUBST,300

BF,ALL,TEMP,TEMP

SAVE
SOLVE

FINISH

/POST1
SET,LAST
ETABLE,SEQV,S,EQV
ETABLE,EL,EPEL,EQV
ETABLE,EP,EPPL,EQV

/OUT,RESULTS
PRETAB,SEQV,EL,EP
/OUT

FINI
EXIT,NOSAVE
```

A.3 Bridgman Notch - Mechanical Load

A.3.1 Linear Elastic Analysis

```
! The following program performs the first linear elastic analysis
! as well as the GLOSS analysis for multiple load cases.


/BATCH


! BRIDGMAN NOTCH - DIMENSIONS


*SET,NR,0.6852E-02        ! NOTCH RADIUS

*SET,OD,2.6416E-02        ! OUTER DIAMETER OF THE NOTCH

*SET,ND,2.1082E-02        ! INNER DIAMETER OF THE NOTCH

*SET,LENG,2*OD            ! LENGTH OF THE NOTCH


*SET,XC,ND+NR

*SET,THE1,77.160412

*SET,THE2,THE1/2.0


! MATERIAL PROPERTIES


*SET,YM,1.90E11

*SET,YS,200E06


*SET,YLOAD,77E06    ! LOAD CORRESPONDING TO FIRST YIELD

*SET,LOAD,(140E06 - YLOAD) ! 140E06 IS THE TOTAL LOAD
```

```
/PREP7

ET,1,42,0,0,1     ! ELEMENT - 4 NODED ISOPARAMETRIC (AXISYMMETRIC)
EX,1,YM

K,1,0,0
K,2,ND,0
L,2,1,22,22
K,4,OD,LENG/2
K,5,0,LENG/2
L,4,5,12
L,5,1,12
LOCAL,11,1,XC
K,3,NR,180-THE1
K,6,NR,180-THE2
L,2,6,12
L,6,3,12
CSYS,0
L,3,4,22,22
L,6,5,22,22
K,7,OD,LENG
K,8,0,LENG
L,4,7,10
L,7,8,12
L,8,5,10
```

114

```
A,1,2,6,5
A,5,6,3,4
A,5,4,7,8
AMESH,ALL

NSEL,S,LOC,X,0
D,ALL,UX,0
NALL

NSEL,S,LOC,Y,0
D,ALL,UY,0
NALL

/SOLU
ANTYPE,0

*DO,I,0,9

/SOLU

NSEL,S,LOC,Y,LENG
SF,ALL,PRES,-(YLOAD + I*LOAD/9)
NALL

SAVE
SOLVE
```

```
FINI


C****                        SOFTENING OF YM


/POST1
SET,1,1


ETABLE,SIGC,S,EQV

ETABLE,ELAS,EPEL,EQV


*DIM,DUM2,ARRAY,1

*DIM,DUM3,ARRAY,1

*CFOPEN,RESULT

*GET,STEQ,ELEM,22,ETAB,SIGC ! 22 is the highest stressed element

*GET,ELEQ,ELEM,22,ETAB,ELAS

DUM2(1) = STEQ

DUM3(1) = (ELEQ/1.3)

*SET,NEUBER,DUM2(1)*DUM3(1)/YS

*VWRITE,DUM2(1),DUM3(1),NEUBER

(3X,E15.8,3X,E15.8,8X,E15.8)

*CFCLOS


SAVE


/SYS,CAT RESULT >> SOLUTION
```

```
*CFOPEN,EXVAL


*SET,MN,2
*GET,K,ELEM,0,COUNT

*DO,L,1,K
*GET,STEQ,ELEM,L,ETAB,SIGC
*IF,STEQ,GT,YS,THEN
*SET,ESEC,((2*YS/STEQ) - 1)*YM
*CFWRITE,MP,EX,MN,ESEC
*CFWRITE,MP,NUXY,MN,0.3
*SET,MN,MN+1
*ENDIF
*ENDDO
*CFCLOS
!--------------------------------------------------------------


*SET,MN,2
*CFOPEN,EXMOD
*DO,L,1,K
*GET,STEQ,ELEM,L,ETAB,SIGC
*IF,STEQ,GT,YS,THEN
*CFWRITE,MAT,MN
*CFWRITE,EMODIF,L
*SET,MN,MN+1
*ENDIF
```

```
*ENDDO
*CFCLOS


FINISH


!--------------------------------------------------
!      II - L I N E A R   A N A L Y S I S
!      --------------------------------------------


/PREP7
RESUME


EX,1,YM
NUXY,1,0.3
*USE,EXVAL
*USE,EXMOD
FINISH
/SOLU
SAVE
SOLVE


FINISH


/POST1
*DIM,DUM4,ARRAY,1
*DIM,DUM5,ARRAY,1
```

```
*CFOPEN,RESULT
SET,1,1
ETABLE,SIGC,S,EQV
ETABLE,ELAS,EPEL,EQV
*GET,STEQ,ELEM,22,ETAB,SIGC
*GET,ELEQ,ELEM,22,ETAB,ELAS
*SET,NUXY1,0.3
DUM4(1) = STEQ
DUM5(1) = ELEQ/(1+NUXY1)
*SET,GLOSS,DUM3(1)+(DUM5(1)-DUM3(1))*(DUM2(1)-YS)/(DUM2(1)-DUM4(1))
! The second point strain is reported as the exact strain in the
! GLOSS method with Plasticity Correction
*VWRITE,DUM4(1),DUM5(1),GLOSS
(X,E15.8,3X,E15.8,3X,E15.8)
*CFCLOS
/SYS,CAT RESULT >> SOLUTION


/PREP7


MP,EX,1,YM
MP,NUXY,1,0.3
MPCHG,1,ALL

*SET,DUM2(1)
*SET,DUM3(1)
*SET,DUM4(1)
```

```
*SET,DUM5(1)


SAVE
*ENDDO


FINI
EXIT,NOSAVE
```

A.3.2   Non-Linear Analysis

```
/BATCH


*SET,NR,0.6852e-02
*SET,OD,2.6416e-02
*SET,ND,2.1082e-02
*SET,LENG,2*OD
*SET,XC,ND+NR
*SET,THE1,77.160412
*SET,THE2,THE1/2.0


*SET,YM,1.90E11
*SET,YS,200E06


*SET,YLOAD,70e06
*SET,LOAD,(140E06 - YLOAD)
```

```
/prep7
ET,1,42,0,0,1
EX,1,YM


TB,BKIN,1,1
TBDATA,1,YS,0


K,1,0,0
K,2,ND,0
L,2,1,22,22
K,4,OD,LENG/2
K,5,0,LENG/2
L,4,5,12
L,5,1,12
LOCAL,11,1,XC
K,3,NR,180-THE1
K,6,NR,180-THE2
L,2,6,12
L,6,3,12
CSYS,0
L,3,4,22,22
L,6,5,22,22
K,7,OD,LENG
K,8,0,LENG
L,4,7,10
L,7,8,12
```

```
L,8,5,10
A,1,2,6,5
A,5,6,3,4
A,5,4,7,8
AMESH,ALL

NSEL,S,LOC,X,0
D,ALL,UX,0
NALL

NSEL,S,LOC,Y,0
D,ALL,UY,0
NALL

/SOLU
ANTYPE,0

*DO,I,0,10

NSEL,S,LOC,Y,LENG
SF,ALL,PRES,-(YLOAD + I*LOAD/10)
NALL

SAVE
SOLVE
*ENDDO
```

```
/POST1

*DIM,DUM1,ARRAY,1

*DIM,DUM2,ARRAY,1

*DIM,DUM3,ARRAY,1

*DIM,DUM4,ARRAY,1

*DIM,DUM5,ARRAY,1

*CFOPEN,RESULT

*DO,I,1,11

SET,I,1

ETABLE,SIGC,S,EQV

ETABLE,ELAS,EPEL,EQV

ETABLE,PLAS,EPPL,EQV

*GET,STEQ,ELEM,22,ETAB,SIGC

*GET,ELEQ,ELEM,22,ETAB,ELAS

*GET,PLEQ,ELEM,22,ETAB,PLAS

DUM1(1) = I

DUM2(1) = STEQ

DUM3(1) = (ELEQ/1.3)

DUM4(1) = (PLEQ/1.5)

DUM5(1) = (DUM3(1) + DUM4(1))

*VWRITE,DUM2(1),DUM5(1)

(3X,E15.8,3X,E15.8)

*ENDDO

*CFCLOS
```

```
FINI

EXIT,NOSAVE
```

A.4 Bridgman Notch - Thermal Load

A.4.1 Linear Elastic Analysis

```
/BATCH


*SET,NR,0.6852E-02

*SET,OD,2.6416E-02

*SET,ND,2.1082E-02

*SET,LENG,2*OD

*SET,XC,ND+NR

*SET,THE1,77.160412

*SET,THE2,THE1/2.0


*SET,YM,1.90E11

*SET,YS,200E06

*SET,ALPHA,1.5E-05


*SET,TEMP,55


/PREP7

ET,1,42,0,0,1
```

```
EX,1,YM
ALPX,1,1.5E-05


K,1,0,0
K,2,ND,0
L,2,1,22,22
K,4,OD,LENG/2
K,5,0,LENG/2
L,4,5,12
L,5,1,12
LOCAL,11,1,XC
K,3,NR,180-THE1
K,6,NR,180-THE2
L,2,6,12
L,6,3,12
CSYS,0
L,3,4,22,22
L,6,5,22,22
K,7,OD,LENG
K,8,0,LENG
L,4,7,10
L,7,8,12
L,8,5,10
A,1,2,6,5
A,5,6,3,4
A,5,4,7,8
```

```
AMESH,ALL

NSEL,S,LOC,X,0
D,ALL,UX,0
NALL

NSEL,S,LOC,Y,0
D,ALL,UY,0
NALL

NSEL,S,LOC,Y,LENG
D,ALL,UY,0
NALL

/SOLU
ANTYPE,0

BF,ALL,TEMP,TEMP

SAVE
SOLVE

FINI

/INP,GLOSSMAC
```

A.4.2 Non-Linear Analysis

```
/BATCH


*SET,NR,0.6852E-02

*SET,OD,2.6416E-02

*SET,ND,2.1082E-02

*SET,LENG,2*OD

*SET,XC,ND+NR

*SET,THE1,77.160412

*SET,THE2,THE1/2.0


*SET,YM,1.90E11

*SET,YS,200E06


*SET,TEMP,55


/PREP7

ET,1,42,0,0,1

EX,1,YM

ALPX,1,1.5E-05


TB,BKIN,1,1

TBDATA,1,YS,0


K,1,0,0

K,2,ND,0
```

```
L,2,1,22,22
K,4,OD,LENG/2
K,5,0,LENG/2
L,4,5,12
L,5,1,12
LOCAL,11,1,XC
K,3,NR,180-THE1
K,6,NR,180-THE2
L,2,6,12
L,6,3,12
CSYS,0
L,3,4,22,22
L,6,5,22,22
K,7,OD,LENG
K,8,0,LENG
L,4,7,10
L,7,8,12
L,8,5,10
A,1,2,6,5
A,5,6,3,4
A,5,4,7,8
AMESH,ALL


NSEL,S,LOC,X,0
D,ALL,UX,0
NALL
```

```
NSEL,S,LOC,Y,0
D,ALL,UY,0
NALL


NSEL,S,LOC,Y,LENG
D,ALL,UY,0
NALL


/SOLU
ANTYPE,0


AUTOTS,ON
PRED,ON,,ON
NROPT,1,,OFF
OUTRES,ALL,ALL


TIME,4
NSUBST,300


BF,ALL,TEMP,TEMP


SAVE
SOLVE


/POST1
```

```
SET,LAST

ETABLE,SEQV,S,EQV

ETABLE,EL,EPEL,EQV

ETABLE,EP,EPPL,EQV


/OUT,RESULTS

PRETAB,SEQV,EL,EP

/OUT


FINI

EXIT,NOSAVE
```

A.5 Cylinder with a Circumferential Notch - Mechanical Load

A.5.1 Linear Elastic Analysis

```
\BATCH


*SET,RI,16            ! INNER RADIUS OF THE CYLINDER

*SET,RO,25            ! OUTER RADIUS OF THE CYLINDER

*SET,RN,1             ! NOTCH RADIUS OF THE CYLINDER

*SET,RIN,RI+RN

*SET,LENG,9           ! LENGTH OF THE CYLINDER


! MATERIAL PROPERTIES
```

```
*SET,YM,27.5E06
*SET,YS,29000


/PREP7
ET,1,42,,,1          ! ELEMENT - 4 NODED ISOPARAMETRIC
                     ! (AXISYMMETRIC)
MP,EX,1,YM


K,1,RIN
K,2,RO
L,1,2,10,10
K,3,RO,LENG
L,2,3,10
K,4,RI,LENG
L,3,4,10
K,5,RI,RN
L,5,4,10,10
LOCAL,11,1,RI
K,6,RN,45
L,1,6,10
L,5,6,10
CSYS,0
L,6,3,10,10
A,1,2,3,6
A,6,3,4,5
```

131

```
AMESH,ALL

FINI

/SOLU

ANTYPE,0

NSEL,S,LOC,Y,LENG
D,ALL,UY,0
NALL

NSEL,S,LOC,Y,0
D,ALL,UY,0
NALL

NSEL,S,LOC,X,RI
SF,ALL,PRES,STRS
NALL

CSYS,11
NSEL,S,LOC,X,RN
SF,ALL,PRES,STRS
NALL

CSYS,0
```

```
SAVE
SOLVE
FINI


/INP,GLOSSMAC
```

A.5.2   Non-Linear Analysis

```
/BATCH


*SET,RI,16
*SET,RO,25
*SET,RN,1
*SET,RIN,RI+RN
*SET,LENG,9
*SET,YM,27.5E06
*SET,YS,29000


/PREP7
ET,1,42,,,1
EX,1,YM


TB,BKIN,1
TBDATA,1,YS,0
```

```
K,1,RIN

K,2,RO

L,1,2,10,10

K,3,RO,LENG

L,2,3,10

K,4,RI,LENG

L,3,4,10

K,5,RI,RN

L,5,4,10,10

LOCAL,11,1,RI

K,6,RN,45

L,1,6,10

L,5,6,10

CSYS,0

L,6,3,10,10

A,1,2,3,6

A,6,3,4,5

AMESH,ALL


FINI


/SOLU


ANTYPE,0


NSEL,S,LOC,Y,LENG
```

```
D,ALL,UY,0
NALL


NSEL,S,LOC,Y,0
D,ALL,UY,0
NALL


AUTOTS,ON
PRED,ON,,ON
NROPT,1,,OFF
NSUBST,300
TIME,4


NSEL,S,LOC,X,RI
SF,ALL,PRES,STRS
NALL


CSYS,11
NSEL,S,LOC,X,RN
SF,ALL,PRES,STRS
NALL


CSYS,0


SAVE
SOLVE
```

```
FINI

/POST1
SET,LAST
ETABLE,SEQV,S,EQV
ETABLE,EL,EPEL,EQV
ETABLE,EP,EPPL,EQV

/OUTPUT,STRESS
PRETAB,SEQV,EL,EP
/OUT

FINI
EXIT,NOSAVE
```

A.6 Cylinder with a Circumferential Notch - Combined Loading

A.6.1 Linear Elastic Analysis

```
\BATCH

*SET,RI,16
*SET,RO,25
*SET,RN,1
*SET,RIN,RI+RN
```

```
*SET,LENG,9
*SET,YM,27.5E06
*SET,YS,29000

/PREP7
ET,1,42,,,1
MP,EX,1,YM
MP,ALPX,1,3E-05

K,1,RIN
K,2,RO
L,1,2,10,10
K,3,RO,LENG
L,2,3,10
K,4,RI,LENG
L,3,4,10
K,5,RI,RN
L,5,4,10,10
LOCAL,11,1,RI
K,6,RN,45
L,1,6,10
L,5,6,10
CSYS,0
L,6,3,10,10
A,1,2,3,6
A,6,3,4,5
```

```
AMESH,ALL

FINI

/SOLU

ANTYPE,0

NSEL,S,LOC,Y,LENG
D,ALL,UY,0
NALL

NSEL,S,LOC,Y,0
D,ALL,UY,0
NALL

NSEL,S,LOC,X,RI
SF,ALL,PRES,STRS
NALL

CSYS,11
NSEL,S,LOC,X,RN
SF,ALL,PRES,STRS
NALL

CSYS,0
```

```
BF,ALL,TEMP,25

SAVE
SOLVE
FINI

/INP,GLOSSMAC
```

A.6.2   Non-Linear Analysis

```
/BATCH

*SET,RI,16
*SET,RO,25
*SET,RN,1
*SET,RIN,RI+RN
*SET,LENG,9
*SET,YM,27.5E06
*SET,YS,29000
*SET,ALPX,3E-05

/PREP7
ET,1,42,,,1
MP,EX,1,YM
MP,ALPX,1,ALPX
```

```
TB,BKIN,1

TBDATA,1,YS,0


K,1,RIN

K,2,RO

L,1,2,10,10

K,3,RO,LENG

L,2,3,10

K,4,RI,LENG

L,3,4,10

K,5,RI,RN

L,5,4,10,10

LOCAL,11,1,RI

K,6,RN,45

L,1,6,10

L,5,6,10

CSYS,0

L,6,3,10,10

A,1,2,3,6

A,6,3,4,5

AMESH,ALL


FINI


/SOLU
```

```
ANTYPE,0

NSEL,S,LOC,Y,LENG
D,ALL,UY,0
NALL

NSEL,S,LOC,Y,0
D,ALL,UY,0
NALL

AUTOTS,ON
PRED,ON,,ON
NROPT,1,,OFF
NSUBST,300
TIME,4

NSEL,S,LOC,X,RI
SF,ALL,PRES,STRS
NALL

CSYS,11
NSEL,S,LOC,X,RN
SF,ALL,PRES,STRS
NALL
```

```
CSYS,0

BF,ALL,TEMP,20

SAVE
SOLVE
FINI

/POST1
SET,LAST
ETABLE,SEQV,S,EQV
ETABLE,EL,EPEL,EQV
ETABLE,EP,EPPL,EQV

/OUTPUT,STRESS
PRETAB,SEQV,E1,EP
/OUT

FINI
EXIT,NOSAVE
```

A.7   Steam Turbine Valve Body

A.7.1   Transient Heat Conduction Analysis

```
/BATCH
```

```
/PREP7

ET,1,77,,,1          ! ELEMENT - 6 NODED THERMAL ELEMENT


/INP,OUTPUT,TMP


!   MATERIAL PROPERTIES


MP,KXX,1,38.37
MP,DENS,1,7460.0
MP,C,1,561.03
MP,EX,1,1.8521E11
MP,ALPX,1,1.5022E-05


/INP,NPR             ! NODES ARE SELECTED ON THE INSIDE SURFACE
D,ALL,TEMP,500
NALL


/INP,NPR
SF,ALL,CONV,3000
NALL


/INP,NPR1            ! INSULATED BOUNDARY CONDITIONS ON THE
                     ! OUTER SURFACE
SF,ALL,HFLUX,0
NALL
```

```
FINISH


/SOLU

ANTYPE,TRANS          ! TRANSIENT ANAYSIS


TIMINT,OFF,STRUC      ! NEGLECT DYNAMIC EFFECTS


AUTOTS,ON
OUTRES,NSOL,ALL
KBC,0                 ! APPLY THE TEMPERATURE LINEARLY
TREF,30               ! REFERENCE TEMPERATURE SET TO 30 C
TUNIF,30              ! INITIAL UNIFORM TEMPERATURE SET TO 30 C
DELTIM,1,,30
TIME,1500             ! THE TEMPERATURE IS APPLIED OVER A PERIOD
                      ! OF 1500 SEC
SAVE
SOLVE


! THE ANALYSIS IS CONTINUED TILL THE STEADY STATE IS REACHED


TIMINT,ON
AUTOTS,ON
OUTRES,NSOL,ALL
DELTIM,1,,60
TIME,4000
```

```
SAVE
SOLVE
FINI


! THE NODAL TEMPERATURES ARE STORED IN A FILE TO BE SUPPLIED AS
! BODY FORCE INPUTS TO THE STRUCTUAL ANALYSIS


/POST1
SET,1,LAST
*CFOPEN,TEMP
*GET,K,NODE,0,COUNT
*DO,L,1,K
*GET,TEM,NODE,L,TEMP
*CFWRITE,BF,L,TEMP,TEM
*ENDDO
*CFCLOS


! DETERMINES THE TEMPERATURE DIFFERENCE AT THE CRITICAL SECTION
! AND OUTPUT IS WRITTEN IN A FILE CALLED AS NODALDIFF


/POST26
NSOL,2,333,TEMP
NSOL,3,252,TEMP
ADD,4,2,3,,,,,1,-1
/OUT,NODALDIFF
PRVAR,2,3,4
```

```
/OUT

FINI

EXIT,NOSAVE
```

A.7.2   Linear Elastic Analysis

```
/BATCH

*SET,STRS,10E07
*SET,YS,300E06
*SET,YM,1.8521E11

/PREP7
ET,1,82,,,1

/INP,OUTPUT,TMP

MP,EX,1,1.8521E11
MP,ALPX,1,1.5022E-05

! STRUCTURAL BOUNDARY CONDITIONS

NSEL,S,LOC,Y,-0.210
D,ALL,UY,0
NSEL,ALL
```

```
D,1847,UX,0
D,1987,UX,0
D,1991,UX,0
D,1993,UX,0

FINISH

/SOLU
ANTYPE,STATIC

/INP,NPR            ! APPLY INTERNAL PRESSURE ON THE INSIDE SURFACE
SF,ALL,PRES,9.81E06
NALL

/INP,TEMP           ! APPLY THE TEMPERATURES AS NODAL BODY FORCE

SAVE
SOLVE

FINI

/INP,GLOSSMAC
```

A.7.3 Non-Linear Analysis

```
/BATCH

*SET,STRS,10E07
*SET,YS,300E06
*SET,YM,1.8521E11


/PREP7
ET,1,82,,,1

/INP,OUTPUT,TMP


MP,EX,1,1.8521E11
MP,ALPX,1,1.5022E-05


TB,BKIN,1,1
TBDATA,1,YS,0


! STRUCTURAL BOUNDARY CONDITIONS


NSEL,S,LOC,Y,-0.210
D,ALL,UY,0
NSEL,ALL


D,1847,UX,0
D,1987,UX,0
```

```
D,1991,UX,0
D,1993,UX,0


FINISH


/SOLU
ANTYPE,STATIC


AUTOTS,ON


PRED,ON,,ON
NROPT,1,,OFF
OUTRES,ALL,ALL


NSUBST,300
TIME,4


/INP,NPR
SF,ALL,PRES,9.81E06
NALL


/INP,TEMP


SAVE
SOLVE
```

```
/POST1
SET,LAST
ETABLE,SEQV,S,EQV
ETABLE,EL,EPEL,EQV
ETABLE,EP,EPPL,EQV

/OUT,STRES
PRETAB,SEQV,EL,EP
/OUT

FINI
EXIT,NOSAVE
```

Appendix B

Elastic Modulii Softening Macro for GLOSS Analysis

The following macro written using the ANSYS Parameric Design Language, changes the modulus and Poisson's ratio after the first linear elastic analysis. The macro provides the equivalent stresses and strains as outputs from the analyses in two files stress1 and stress2.

B.1 GLOSS Macro for modulus and Poisson's ration modification

```
!        ---------------------------------------------
!            I - L I N E A R    A N A L Y S I S
!        ---------------------------------------------


!        ******** THIS MACRO IS FOR COMBINED LOADINGS **************


! The parameters YS (yield strength), YM (modulus of elasticity) and
```

```
! ALPHA (co-efficient of thermal expansion) has to be specified in
! the main linear elastic program


/POST1

SET,1,1

ETABLE,SIGC,S,EQV

ETABLE,EIGC,EPTO,EQV


/output,stress1

PRETAB,SIGC,EIGC

/output


!c****                SOFTENING OF YM


*CFOPEN,EXVAL


*SET,MN,2

*GET,K,ELEM,0,COUNT


*DO,L,1,K

*GET,STEQ,ELEM,L,ETAB,SIGC

*IF,STEQ,GT,YS,THEN

*SET,ESEC,((2*YS/STEQ) - 1)*YM

*CFWRITE,MP,EX,MN,ESEC

*CFWRITE,MP,ALPX,MN,ALPHA
```

```
*CFWRITE,MP,NUXY,MN,0.499
*SET,MN,MN+1
*ENDIF
*ENDDO
*CFCLOS
!----------------------------------------------------------------


*SET,MN,2
*CFOPEN,EXMOD
*DO,L,1,K
*GET,STEQ,ELEM,L,ETAB,SIGC
*IF,STEQ,GT,YS,THEN
*CFWRITE,MAT,MN
*CFWRITE,EMODIF,L
*SET,MN,MN+1
*ENDIF
*ENDDO
*CFCLOS


FINISH


!----------------------------------------------------------------
!       II - L I N E A R    A N A L Y S I S
!       ------------------------------------------------


/PREP7
```

```
RESUME

EX,1,YM
ALPX,1,ALPHA
*USE,EXVAL
*USE,EXMOD
FINISH

/SOLU
SAVE
SOLVE
FINISH

/POST1

SET,1,1
ETABLE,SIGC,S,EQV
ETABLE,EIGC,EPTO,EQV

/output,stress2
PRETAB,SIGC,EIGC
/output

FINISH
```

B.2 Macro for scaling stresses and strains to obtain the relaxation locus

```
*DIM,DUM1,ARRAY,1

*DIM,DUM2,ARRAY,1

*DIM,DUM3,ARRAY,1

*DIM,DUM4,ARRAY,1

*DIM,DUM5,ARRAY,1

*CFOPEN,RESULT

*DO,I,1,20                    ! The number of uniform load steps

SET,I,1

ETABLE,SIGC,S,EQV

ETABLE,ELAS,EPEL,EQV

ETABLE,PLAS,EPPL,EQV

*GET,STEQ,ELEM,1,ETAB,SIGC  ! 1 corresponds to the local element

*GET,ELEQ,ELEM,1,ETAB,ELAS

*GET,PLEQ,ELEM,1,ETAB,PLAS

DUM1(1) = I

DUM2(1) = 20*STEQ/I

DUM3(1) = (ELEQ/1.3)

DUM4(1) = (PLEQ/1.5)

DUM5(1) = 20*(DUM3(1) + DUM4(1))/I

*VWRITE,DUM5(1),DUM2(1)

(3X,E15.8,3X,E15.8)

*ENDDO

*CFCLOS
```

Appendix C

Strain Calculations in ANSYS

The total equivalent strain is the sum of elastic equivalent strain and the plastic equivalent strain. In a general form, the equivalent strain is given by

$$\epsilon_{eqv} = \frac{1}{\sqrt{2}\,(1+\nu)} \sqrt{\left[(\epsilon_1 - \epsilon_2)^2 + (\epsilon_2 - \epsilon_3)^2 + (\epsilon_3 - \epsilon_1)^2\right]} \qquad (C.1)$$

The equivalent strain values obtained from ANSYS does not consider the Poisson's ratio factor. Therefore, elastic equivalent strain values obtained using EPEL,EQV command should be divided by 1.3 in order to get the correct elastic equivalent strain. Similarly, plastic equivalent strain values obtained using EPPL,EQV command (used in non-linear analysis) should be divided by 1.5 in order to get the correct plastic equivalent strain. Their sum gives the required total equivalent strain.

In the GLOSS analysis, the strain values obtained using EPEL,EQV command has to corrected according to the elements Poisson's ratio.